WIND TUNNEL PRESSURE MEASUREMENTS ON THE AYLESBURY LOW-RISE HOUSING ESTATE

Part 1

Simulation Design and Mean Pressures

M. E. Greenway and C. J. Wood

OUEL Report No. 1213/77

CONTENTS

1. INTRODUCTION

This report describes the first stage of an investigation which is in progress in the Oxford University 4m x 2 m industrial aerodynamics wind tunnel and which is due to be completed in the autumn of 1978. It is one of several parallel investigations designed to provide wind tunnel data for comparison with the recently completed full-scale tests by the Building Research Establishment on the Grenville Green housing estate at Aylesbury (Eaton & Mayne 1975, Eaton, Mayne and Cook 1976).

The Grenville Green estate, shown in Figs. 1 and 2 features six parallel rows of two-storey terraced houses aligned at 332^{o} relative to true north. The prevailing south-westerly winds thus blow across the estate approximately at right angles to the building rows.

In addition to the estate houses, a specially built test house with a variable pitch roof was sited to the west of the estate as shown in Fig. 2. Close to the test house a 20m high mast carried a wind vane and several cup anemometers to monitor the incident wind during tests.

Pressure measurements on the estate were made by flush-mounted diaphragm transducers. The backing pressure for these transducers, which therefore became the reference pressure for all measurements, was derived from tubed connections of considerable length to a small underground cavity, approximately $1\Delta m^3$ in volume, vented by a small hole to ground level in a field between the test house and the first row of estate houses. By virtue of the cavity volume and the damping effect of the connecting tubes, the reference pressure was presumed to be steady although the actual time-constant does not appear to have been measured.

Data published from these tests include mean pressures, variable and peak values as well as power-spectral density distributions for strong winds from various directions.

In the present wind tunnel study it was decided to concentrate first

upon the prevailing south-westerly wind direction for which the approaching wind passed over an uninterrupted fetch of open farmland. The present report therefore describes the development of a single wind simulation appropriate to this terrain together with the first stage of the pressure measurements leading to a comparison of mean pressures.

Other wind tunnel measurements on this estate have been reported by Bray (1977) at the University of Bristol and by Apperley of the University of Sydney, working at the University of Western Ontario. In addition, the authors understand that similar experiments are being conducted by Gardener at C.S.T.B. Nantes, by Holmes at the University of Queensland and by Cook at the Building Research Establishment, Garston.

It is anticipated that the comparison of results from these various facilities, as they become available, together with the full-scale data already collected will help to provide the experience necessary for making realistic appraisals of the significance of measured data both at model scale and at full scale. It could also lead to useful improvements in technique.

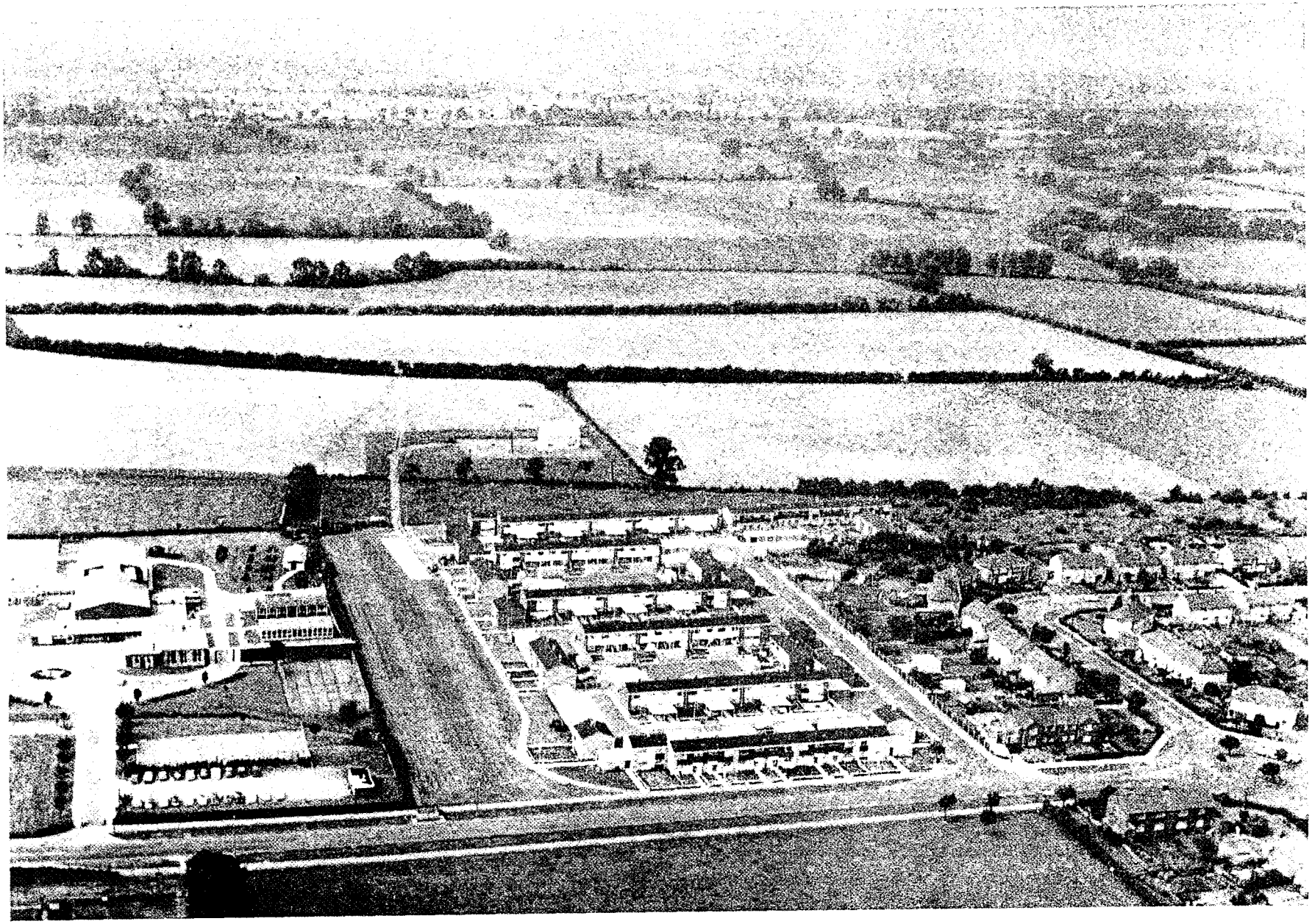

Fig. 1 Aerial View of Grenville Green looking West

2. THE WIND TUNNEL

The new 4m x 2m low speed wind tunnel, which was completed at the Oxford University Engineering Laboratory in 1974, has been described fully by Wood (1977). It is an open-return tunnel with a contraction of area ratio 2.8 leading to a 14m long working section. The flow is divided downstream of the working section and is carried by two diffusers of area ratio 1.54 with 3.5 degrees equivalent cone angle to a pair of Woods 280-JG-71/10/20 variable pitch, 16 bladed axial fans.

A pole-changing system on the induction motors provides two alternative fan speeds of 594 r.p.m. or 296 r.p.m. while a specially designed control system varies the pitch of the two fans in common mode and in differential mode to provide any selected wind speed from 0 to 30m s^{-1} (empty tunnel) with a balanced flow in the diffusers.

3. INSTRUMENTATION AND DATA PROCESSING

For velocity measurements, two Disa K series hot wire anemometers were available. However, where dynamic pressures rather than velocities were required a pilot-state tube was often found more convenient.

The basic instrumentation used for the pressure measurements consists of two DISA miniature pressure transducers based upon the B & K $\frac{1}{4}$ inch capacitance microphone. Where frequency response was not a limiting factor, these could be mounted in Type D, 48 port, solenoid driven Scanivalves. Alternatively they could be mounted directly in special low-volume adapters either inserted in individual surface pressure drillings or connected to them by short lengths of flexible tube.

The DISA transducer system operates by using capacitance changes in the miniature microphone to vary the frequency of a sensitive oscillator. A reactance convertor then produces an analogue voltage output. Calibration against a Betz micromanometer showed that the voltage output was linear with an extremely stable slope which, on the sensitive range used in the present tests, approached 160 Nm^{-2} per Volt so that pressure changes of 1 Nm^{-2} were easily detected. With its high frequency response it was thus an ideal instrument for measuring small oscillating pressure signals.

When used for mean pressure measurements however, at the low signal levels found in the present experiments a serious difficulty is caused by the relatively large and random zero-drift rates. Zero-drift is caused partly by the temperature sensitivity of the oscillator frequency and partly by the fact that capacitance changes caused by small displacements of the short co-axial microphone cable are not small compared with the pressure-induced capacitance changes in the microphone itself. The instrument is therefore extremely sensitive to vibration.

In mounting the transducers therefore, for mean pressure measurements in particular, the whole transducer unit, including the oscillator and the connecting cable was sandwiched tightly between encasing blocks of expanded

polystyrene. The scanivalve was also encased in the same block but to prevent the transmission of vibration caused by the operation of the stepping soleniod, the microphone was not mounted in the scanivalve body as is ususal. Instead it was connected to the common pressure by means of special adaptor and a very short flexible tube.

It must be emphasized of course that this mode of operation reduced the frequency response of the system and was therefore used only for mean-pressure measurements.

For signal conditioning, a dual-channel Kemo switchable filter was provided. Also, D.C. preamplifiers were used to adjust the level of the output signals from the velocity and pressure transducers before connecting them to the analogue-digital converter of a PDP 11/10 computer which is situated close to the wind tunnel.

Subject to the needs of other users of the shared computing facility, the majority of the data reduction programmes written for these experiments are capable of producing numerical results in real time and returning them to a teleprinter in the tunnel control cabin as each run progresses. Graph plotting being a little slower, is normally done later, although an oscilloscope is used for an instantaneous display where necessary.

The computer itself was not available at the start of the project and initial measurements were taken using instead a Hewlett-Packard Correlator kindly loaned by Mr. T. V. Lawson of the University of Bristol. From the correlation, with the aid of a tape punch interface, 100 point probability density distributions and autocorrelation functions were transferred on paper tape to the Oxford University I.C.L. 1906 computer for further processing.

After the necessary software for the PDP 11 had been prepared and before the correlator was returned it was verified that the two data processing systems were producing consistent results.

4. THE MODEL

The availability of a 3.5 m diameter turntable near the downstream end of the working section led to the choice of a model scale of 1/75. As shown in Figs. 2 and 3 this allows the whole of the relevant part of the estate to be mounted on the turntable.

The houses were constructed of 3 mm plywood to plans supplied by the Building Research Establishment. This construction allowed the removal of whole houses or of individual panels for the insertion of pressure transducers or connecting tubes.

The tubes used were approximately 1.5 mm in diameter and were carefully finished flush with the external surface of the models after insertion.

Taking advantage of the deliberately recessed design of the turntable, the model was assembled on a set of removable chip-board panels. When these were mounted in the tunnel, the ground surface was flush with the tunnel floor, while there remained space underneath for instrumentation.

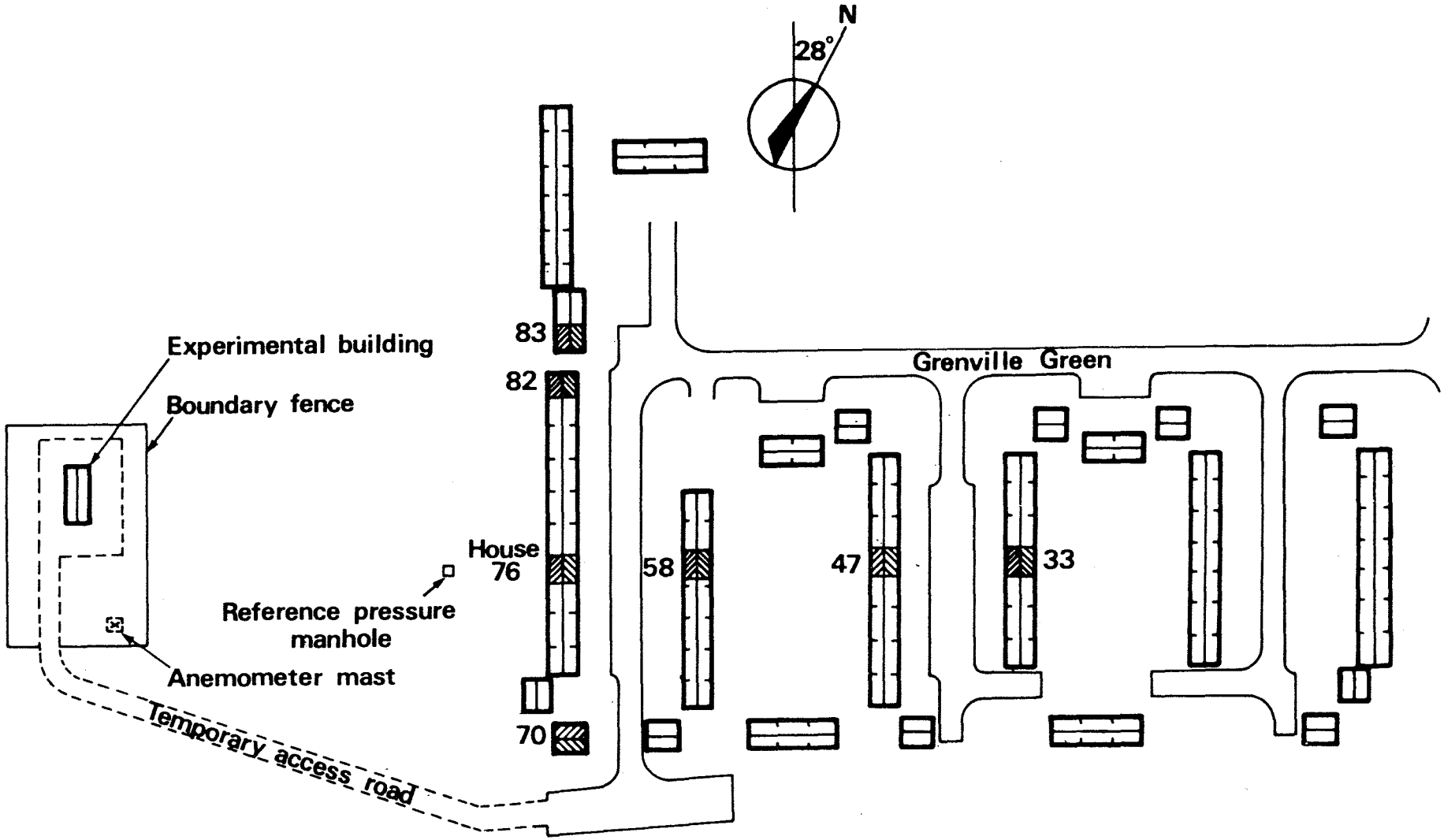

Figure 2 Plan of Aylesbury site

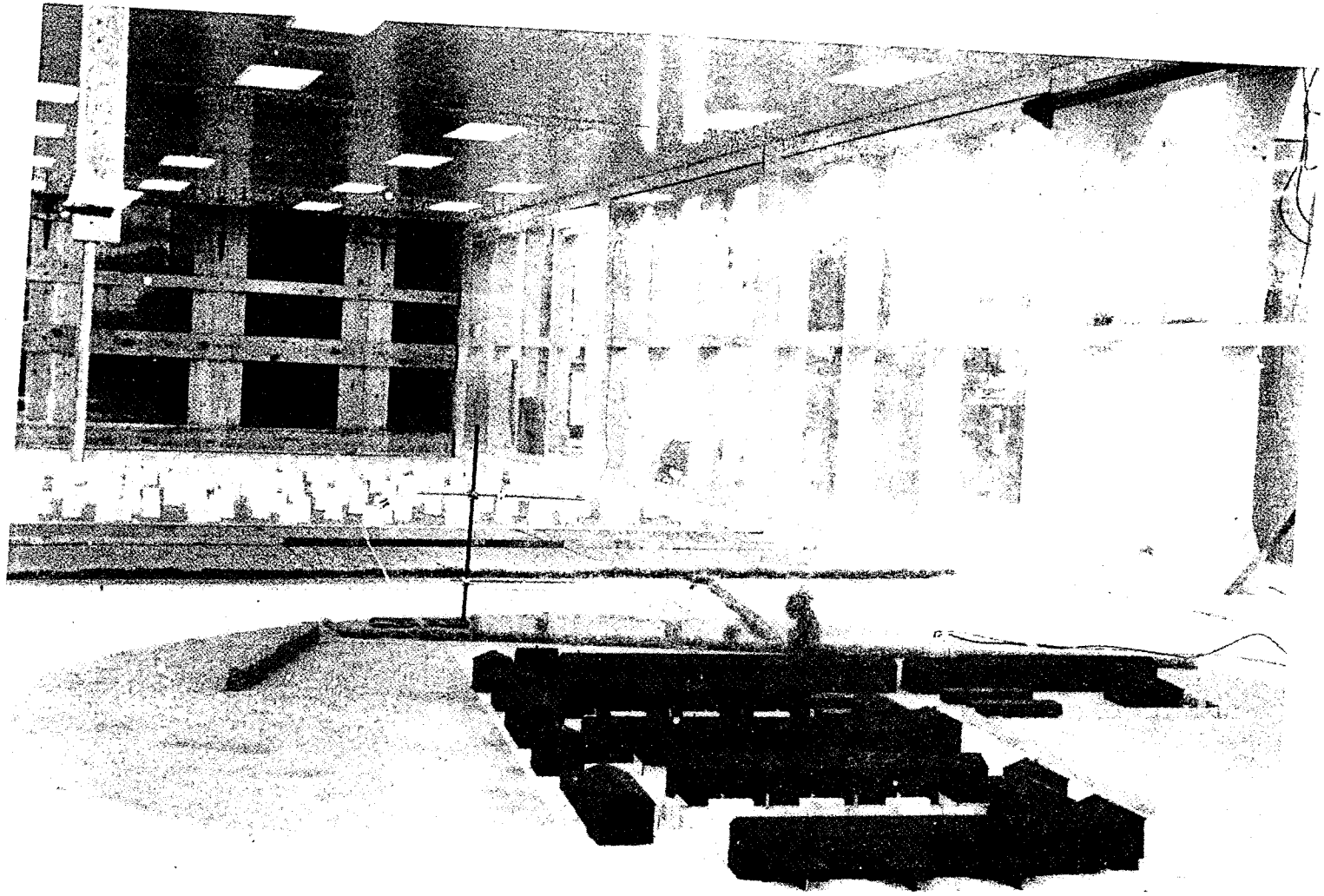

Fig. 3 Estate Model in Wind Tunnel

5. WIND SIMULATION DESIGN

5.1 General Discussion

The parameters used to describe the structure of turbulent wind flow are merely statistical descriptions. This is unavoidable and the number required for a complete description is large and indeterminate. The number of parameters used in practice depends upon the level of description which is thought necessary. The current state of opinion in architectural aerodynamics is that an absolute minimum description must include not only the mean velocity profile but also the distribution of turbulence intensity (for longitudinal components at least) together with spectral information to describe the frequencies present.

Because the flow of strong winds over the earth have distributions of mean velocity and turbulence which are similar to those found in turbulent boundary layers elsewhere, it is normally accepted that the best wind tunnel simulation for strong winds must be generated by the natural growth of a turbulent boundary layer. This philosophy permits the reassuring presumption that a simulation in which the basic parameters listed above have been matched to the prototype, is in fact a better simulation than it appears to be. This is because it has the same fundamental nature as the prototype flow and is therefore likely to exhibit corresponding values of other parameters. e.g. Reynold's stress distribution perhaps, which are not in fact measured.

The ideal of a naturally grown boundary layer is often found to be impractical however, because of the excessive tunnel length required to grow a boundary layer of sufficient thickness. The next best approach is to induce the accelerated growth of the required boundary layer over a shorter fetch of wall roughness.

To achieve this, an artificial input of shear and turbulence

is provided at the upstream end which, although it is expected to decay and play very little part in the structure of the final flow, has the effect of promoting the rapid diffusion of the required characteristics generated by the rough wall. This argument forms the basis for many of the accelerated growth methods described for example by Counihan (1969) or Cook (1973).

5.2 Selection of a Simulation Target

During the full-scale experiments at Aylesbury the wind speed was recorded continuously at heights of 1.5 m, 5 m, 10 m, 15 m and 20 m above ground level. 30 minute mean values are quoted by Eaton & Mayne (1974) together with turbulence intensity measurements and frequency spectra at 3 m, 5 m and 10 m. The cup anemometers employed in this work had a high frequency cut-off at about 0.5 hz.

The results of these measurements are reproduced in Figs. 4 and 5. Also shown are curves derived from wind speed data supplied by the Engineering Sciences Data Unit (E.S.D.U. 1972, 1974).

In selecting the E.S.D.U. data most appropriate to the Aylesbury site it was noted that the prevailing westerly winds approach the site over several kilometres of level, open farmland (Fig. 1). For this terrain the empirical roughnessfactor z_o in the logarithmic velocity profile was estimated to be 0.07 m (Bray (1977) chose 0.1 m, see below). The zero-plane displacement d was taken to be zero.

It is clear from Figs. 4 and 5 that there is rather poor agreement between the E.S.D.U. data, which represents the average of a large number of collected measurements, and the particular flow found at the Aylesbury site. This discrepancy not only draws attention to the large scatter which is a feature of much full-scale data, but in the present context it also raises a fundamental question about the basic philosophy of designing wind tunnel simulations.

FIG 4

COMPARISON OF MEAN VELOCITY PROFILES

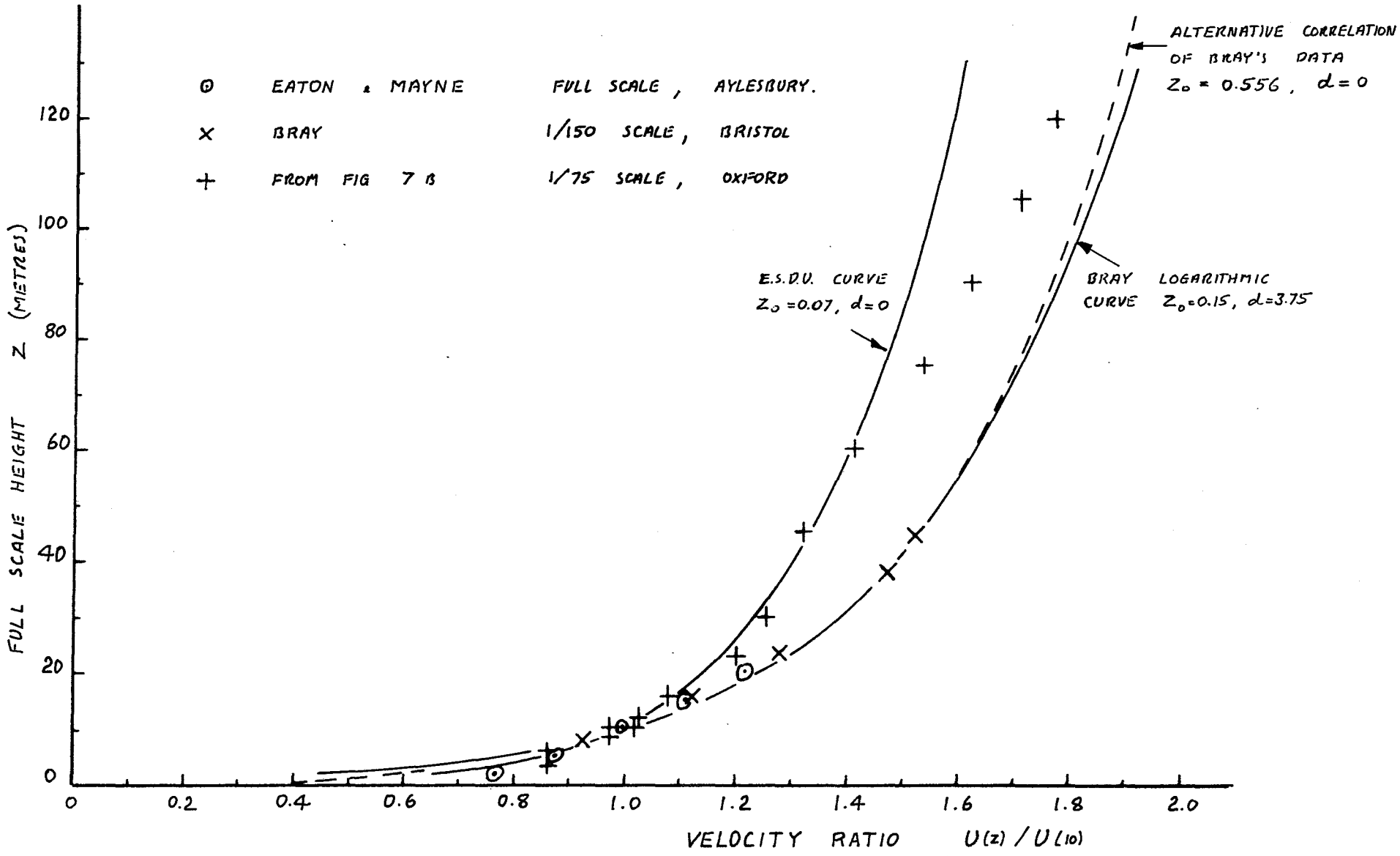

FIG 5

COMPARISON OF POWER SPECTRA FOR LONGITUDINAL VELOCITY AT 10 M

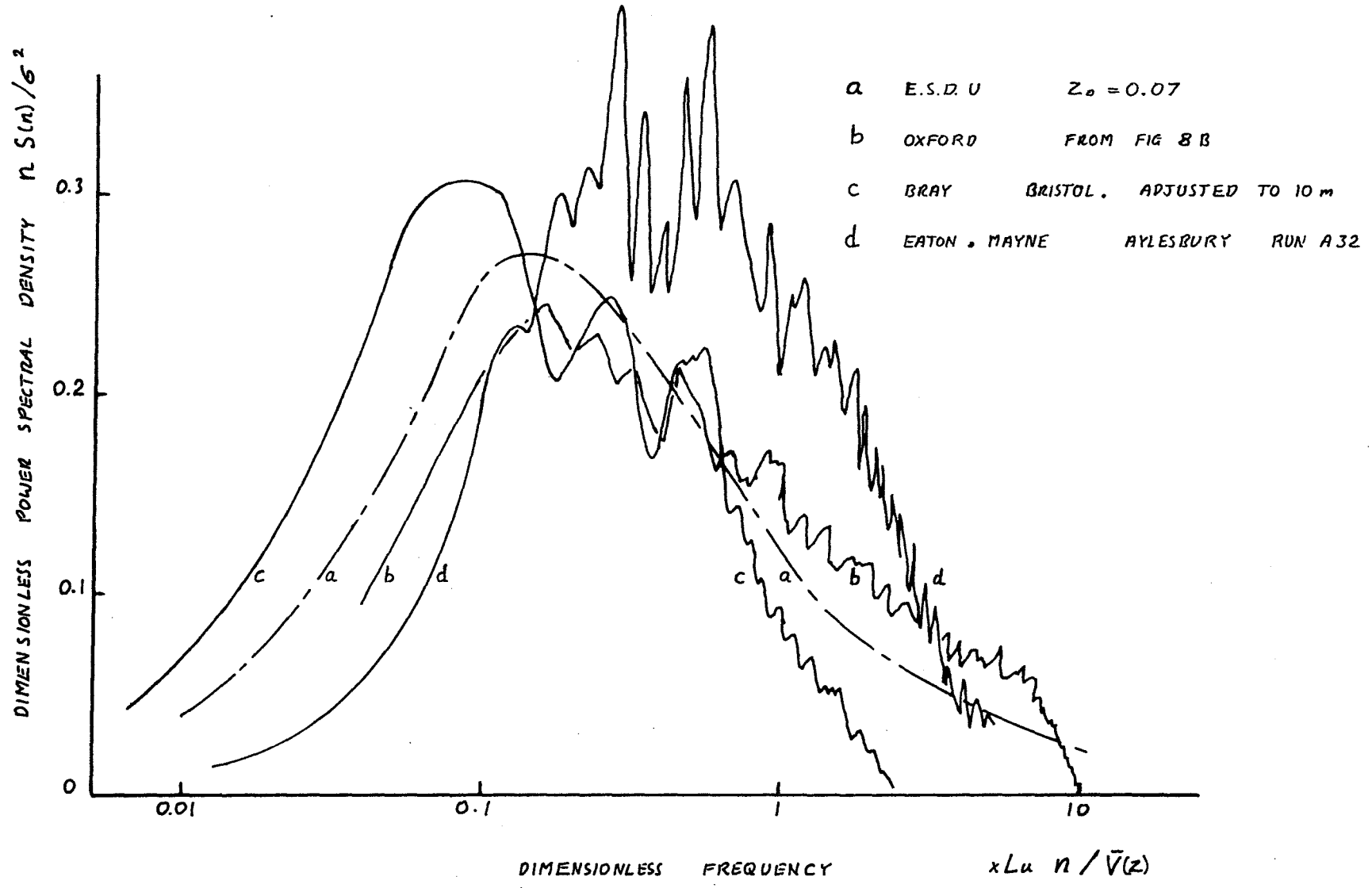

At first sight it would appear to be better, where such data is available, to simulate as far as possible the locally measured wind conditions affecting the site under investigation. However, in most situations such data is not available so that the local wind characteristics must be regarded as part of the prediction problem and not as input data.

It is for precisely this reason that the Engineering Sciences Data Unit (E.S.D.U. 1972, 1974) and others have attempted to provide universal correlations of wind data from which nominal or standard local conditions can be predicted. For this reason also, since the present experiments are intended in part to be a realistic assessment of wind tunnel technique, the present authors have ignored the measured Aylesbury wind structure and have sought instead to reproduce in the wind tunnel a standard wind for the site based upon the E.S.D.U. data sheets.

If time permits towards the close of the present investigation, it is planned to consider a little more closely the effect of wind simulation errors by repeating some of the pressure measurements with one or more deliberately distorted wind structures.

5.3 Simulation Devices

At the present scale of 1/75 the 2 m height of the wind tunnel permits the simulation of the wind structure up to a height of only 150 m. As this is less than the total thickness of the wind boundary layer it was necessary to use a part-depth simulation for the present experiments.

As an initial approach, the system favoured by Cook (1973) was installed. A regular grid of 210 mm wide bars with a solidity of 0.6 was mounted close to the working section inlet 11.4 m from the turntable centre. This was followed by a variable height fence at 10.5 m and a pseudo-random array of 93 mm plastic coffee cups at a volume density of 0.07 was laid to cover the tunnel floor from 9.8 m to 2.4 m.

At this stage the arrangement was entirely arbitrary. There followed a typically tedious sequence of trial-and-error modifications with the object of producing a flow having the required mean velocity profile, turbulence

intensity and frequency spectrum. At the close of this phase of the work the regular grid had been abandoned in favour of a vertically graded grid at 12.0 m. Even after 10 m or more of the settling length, it was found that the turbulence length scales were still influenced by the grid bar dimensions and a useful reduction in frequency was obtained by combining the six original vertical bars to form three bars each 420 mm wide.

Curiously, the widened grid bars were found to be incompatible with the close proximity of the momentum fence downstream. Within the extensive near wakes of the bars a strong vertical flow transported large quantities of low momentum air from the stagnation region ahead of the fence and dispersed it near the tunnel roof. This flow was controlled by adjusting the streamwise position of the fence until it was virtually incorporated in the grid itself, being separated only by a carefully adjusted spacer as shown in Fig. 6.

The removal of the fence, with its associated wake separation region, allowed more effective use of the upstream part of the floor roughness. The downstream section was eventually removed leaving the coffee cup array only between 9.8 m and 5.0 m. This allowed a more extensive modelling of the farmland terrain upstream of the turntable. Details were not included but a set of 33 mm wooden fences spaced 1 m apart were inserted to generate the effect of fields with low hedges. This produced an immediate improvement in the shape of the mean velocity profile at low level which had previously been affected excessively by the wakes of the roughness elements close upstream.

For some of the measurements described below the array of fences was extended over the turntable surface after removing the model. The layout is shown in Fig. 6.

For the final simulation as used throughout the present tests, the 33 mm fence at 2.73 m was removed and replaced by a model of the actual hedge layout as deduced from aerial photographs (e.g. Fig. 1). The hedges

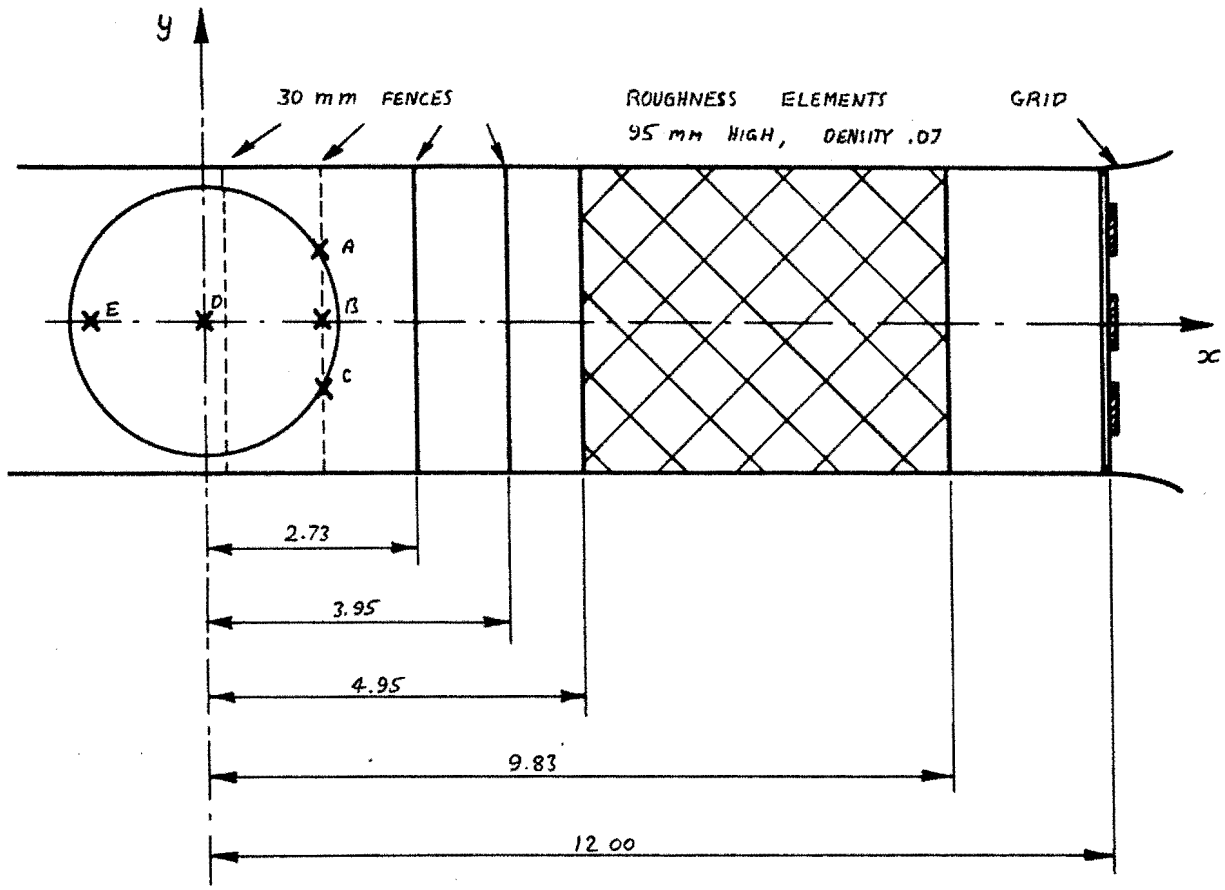

FIG 6 A

PLAN OF SIMULATION DEVICES FOR 1/75 SCALE, $Z_o = 0.07$ m

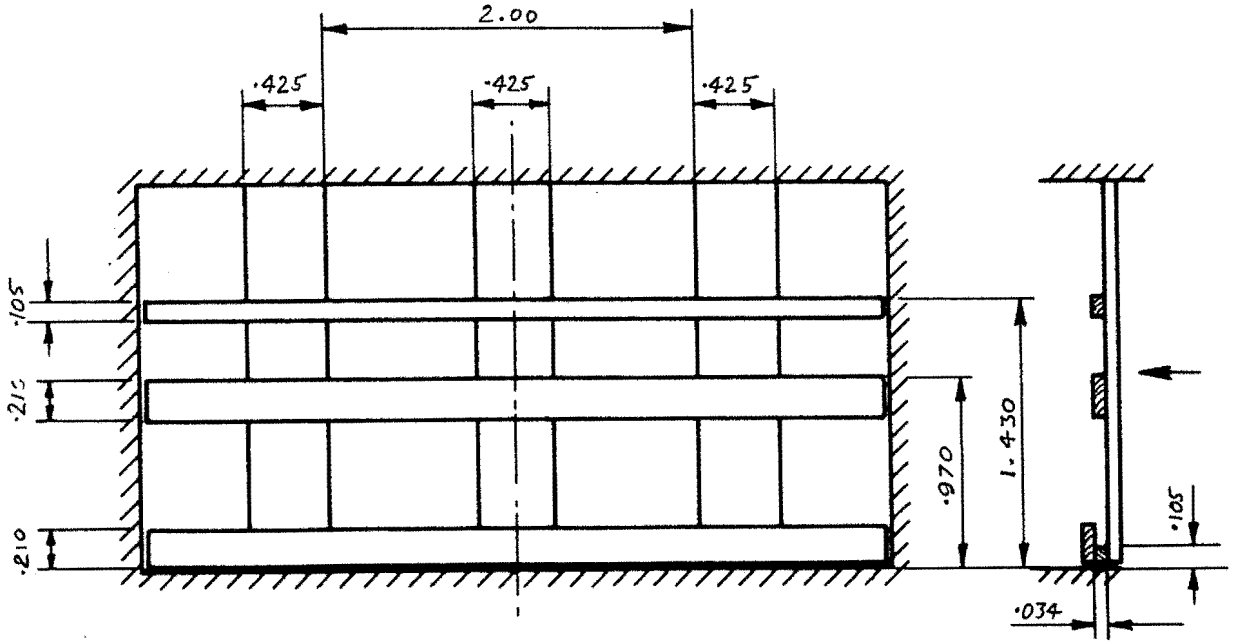

FIG 6 B

DIMENSIONS OF GRADED GRID FOR 1/75 SCALE, $Z_o = 0.07$ m

and any salient trees were formed by trimming strips of "Hairlock" rubberised hair matting. They were pinned in positions appropriate to the 235° wind direction selected (see section 6 below). By representing more accurately the porous nature of the hedges, this alteration produced a further slight improvement in the velocity profile and turbulence levels near the ground upstream of the turntable.

5.4 Comment on Limitations

It is obvious from the foregoing description of the simulation development work that there remains very little justification for any claim that the final flow represents a natural turbulent boundary layer. At the present scale of 1/75 the 12 m fetch in the working section is simply not long enough to allow the effects of the grid to disappear and the characteristics appropriate to the roughness array to predominate.

Thus although the resulting flow, which is described below, has approximately the desired distributions of mean velocity and longitudinal turbulence intensity over the whole turntable area as well as good frequency characteristics, it must be declared that this is a flow in which only those particular characteristics have been measured. Because it seems not to be a true equilibrium boundary layer it does not necessarily follow that other unmeasured properties are equally well simulated. This is an acknowledged limitation of the present experiment.

5.5 Measurements

In order to measure the velocity profiles, one of the two hot-wire anemometer probes was mounted at a series of positions along a slender vertical pole set at the chosen station. Until confidence was gained in the tunnel speed control system, which was under development at the time (Wood, 1977) a second anemometer was held in a fixed position elsewhere in the tunnel as a reference to guard against errors arising from changes in the tunnel speed during a traverse. Any such effects were eliminated by recording mean velocities alternately from the traversing probe and the reference probe. Each mean velocity in the traverse was then divided by the mean of the

immediately preceding and subsequent reference velocities to give a dimensionless relative velocity. Later the relative velocity obtained at 0.133 m (10 m full scale) was used to scale the whole profile to the E.S.D.U. format. In this procedure the probe calibration was unimportant.

With a low-pass analogue filter set at 50 Hz each channel was sampled at 100 Hz for periods around 50 seconds sufficient to build a probability density distribution. The growth of these were monitored, using the dynamic visual display facility, as a check against distortions which would have indicated the occurrence of values which were either out of range for the A.D.C. or negative.

From the first and second moments of these distributions the mean velocities and turbulence intensity values were computed. Third and fourth moments were also recorded together with quantiles at 0.99 and 0.01.

Profiles were measured, with the model removal, at each of the five traverse stations marked a, b, c, d and e in Fig. 6. These profiles are shown in Fig. 7 a to e.

The power spectral density measurements, shown for the five measuring stations in Fig. 8 were made with a single hot wire probe fixed at a height of 133 mm (equivalent to 10 m full scale) above the turntable surface. The computing procedure for a typical spectrum was to collect 112 separate blocks of data each containing 512 instantaneous velocity readings taken at intervals of 8 ms. The sampling frequency and the number of samples in each set were chosen to yield a frequency range from 0.244 Hz to 62.5 Hz in the resulting spectrum.

To correspond with these frequencies, analogue filter settings were made to pass signal components between 0.1 Hz and 50 Hz thus eliminating the mean value and avoiding high frequency aliasing problems.

By applying a discrete Fourier Transform to each data block (a standard Fast Fourier Transform routine was used in the computer), a set of real and imaginary Fourier coefficients was obtained. These were then combined to yield the ordinates for a power-spectral density curve of the type shown in

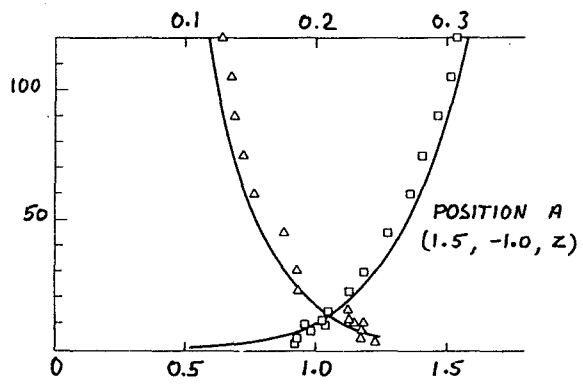

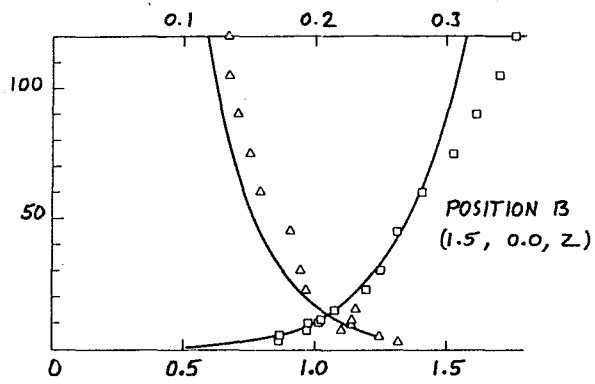

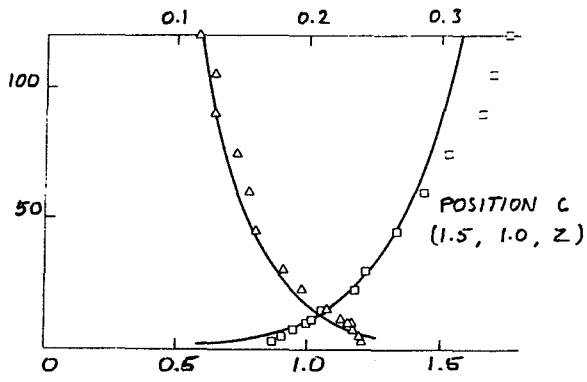

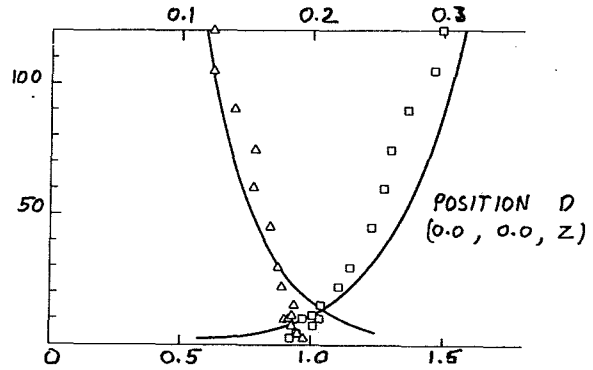

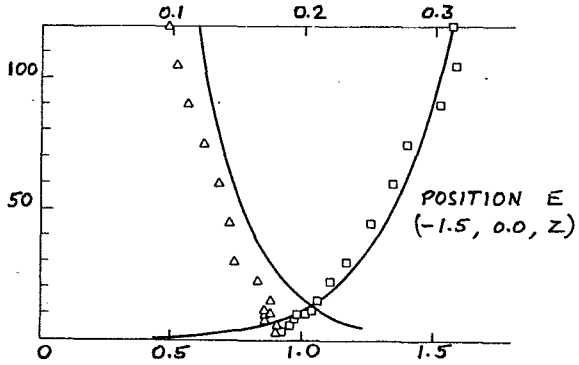

FIG 7

MEAN VELOCITY AND TURBULENCE INTENSITY PROFILES

△ TURBULENCE INTENSITY $\sigma(z)/V(z)$ (UPPER SCALES)

□ VELOCITY RATIO $V(z)/V(10)$ (LOWER SCALES)

HEIGHTS IN METRES (FULL-SCALE)

POSITION COORDINATES IN METRES FROM TURNTABLE CENTRE (FIG 6)

SOLID CURVES REPRESENT E.S.D.U.

DATA FOR $Z_0 = 0.07$ M $d = 0$

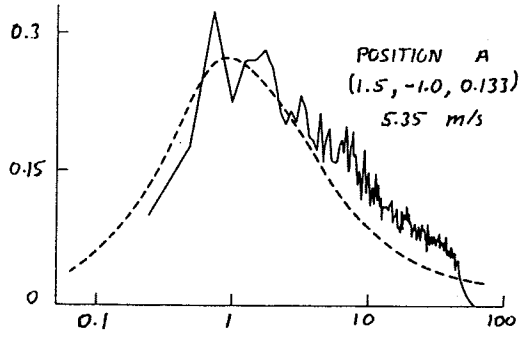

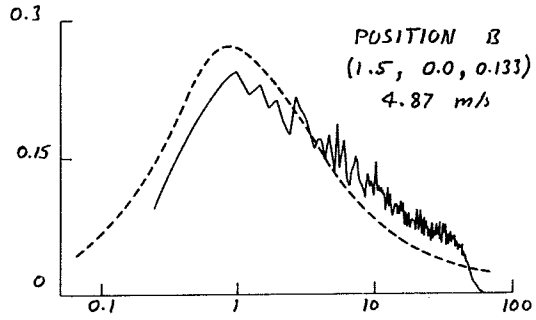

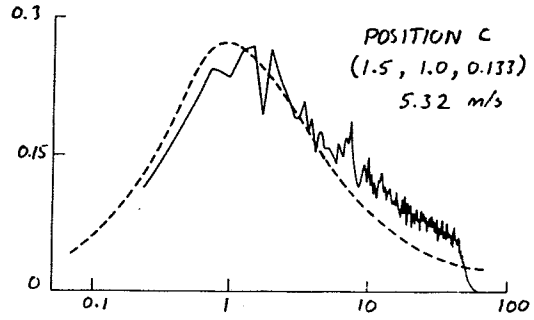

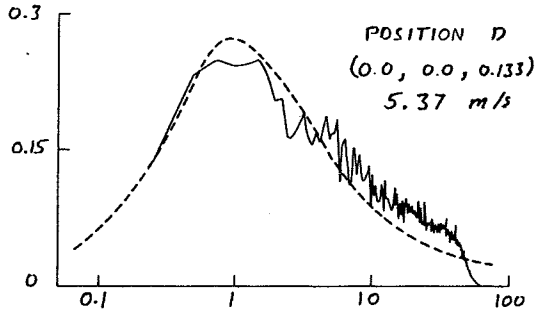

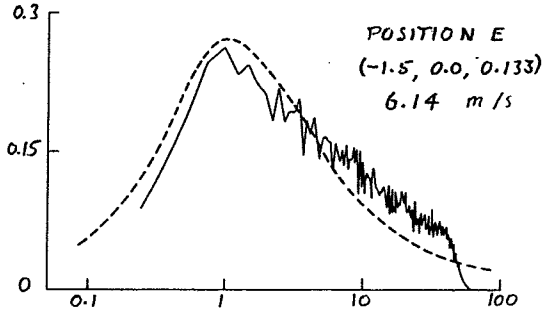

FIG 8

DIMENSIONLESS POWER SPECTRAL DENSITY ($n S_p / \sigma^2$) PLOTS FOR LONGITUDINAL VELOCITY

FREQUENCIES ARE IN Hz AT MODEL SCALE

POSITION COORDINATES IN METRES RELATIVE TO TURNTABLE CENTRE (FIG 6)

DOTTED CURVES REPRESENT E.S.D.U DATA FOR $Z = 0.07$ m. $d = 0$

Fig. 8. To obtain the final smoothed spectrum for each case, the results from the 112 separate blocks were averaged.

As already stated in section 3, the spectra obtained by this method of averaging in the frequency domain compared very favourably with those obtained in tests using the Hewlett-Packard Correlator simultaneously. This produced a time-averaged autocorrelation function, from which a single transformation yielded the power spectrum.

Examining the uniformity of the flow over the turntable area by means of Figs. 7 and 8, it is clear that, despite the suspected non-equlibrium nature of the flow, no serious relaxation appears to occur.

Fig. 7 shows good agreement with the E.S.D.U. "target" distributions for the transverse row a, b, c of stations 1.5 m upstream of the turntable centre. Traverse e, 3 m further downstream shows the extent to which the turbulence intensity has decayed and also shows how the ground-level velocity has tended to increase over the smooth turntable surface. This occurrs despite the insertion of an extra 33 mm fence across the empty turntable to maintain the hedge/field simulation.

Traverse d, taken over the turntable centre is spoiled by the proximity of this additional fence 0.3 m upstream. Because the profile is referred to the 10 m (0.133 m) velocity which is itself in the affected region the whole profile appears to be shifted. If local influences are to be recognised more clearly, there is obviously a case for abandoning the E.S.D.U. format here and taking an undisturbed reference higher in the profile.

Turning to Fig. 8 and examining the five frequency spectra it appears that the tunnel frequencies are a little high at the upstream edge of the turntable. However the agreement with the E.S.D.U. "target" curves tends to improve further downstream. In making such comparisons it should be remembered that the standard E.S.D.U. curves are based upon data which is sparse and also very variable due to the difficulties in making experimental measurements in the full-scale wind. Agreement within a frequency spread of

± 30 per cent is in fact well within the scatter of full scale data.

5.6 Comparison with other investigations

Comparing the present simulation with that used by others participating in the Aylesbury project it is noted that the decision to simulate a standard E.S.D.U. wind structure was also taken by Bray 1977. He selected a value of 0.1 m for the surface roughness length z_o which is close to the present choice of 0.07 m. However, in designing his 1/150 scale simulation, Bray appears to have actually used a value of 1 mm for z_o at model scale, which corresponds to 0.15 m at full scale. In addition, having failed to produce an experimental mean velocity profile to match his target curve, he then adjusted his target curve to fit his experimental data by choosing a value of 3.75 m (full scale) for the zero plane displacement d although this is normally taken to be zero for rural terrain (E.S.D.U. 1972). It is shown in Fig. 4 that this adjustment of d is approximately equivalent to a choice of 0.56 m for z_o with d = 0; a value more appropriate to the centre of a small town than to rural terrain (E.S.D.U. 1972).

By a curious and not inconvenient coincidence, the nett result of these changes is a mean velocity profile which matches very closely the measured full-scale velocity profile of Eaton and Mayne (1975) rather than the intended E.S.D.U. profile. In comparing the results of the Bristol and Oxford wind tunnel tests it may be possible therefore to gain some impression of the effect of velocity profile discrepancies.

Turbulence intensity profiles are not given by either Bray (1977) or by Eaton and Mayne (1975). Consequently a comparison is possible only at the one height (10 m) for which values are available from all three experiments. The agreement shown in Table 1 is remarkable.

Power spectral density curves again cannot be compared directly because Bray's (1977) result from the Bristol simulation is taken at a height of 45 m whereas the Oxford and B.R.E. full-scale results are quoted at 10 m. However, if a common value of 0.07 is assumed arbitrarily for z_o, together

TABLE 1

Comparison of Longitudinal Turbulence Intensities at 10 m

Source	$\sigma_u/\bar{V}_{10}$
B.R.E. (Run A7)	0.23
Bristol (Rural Simulation)	0.23
Oxford (From Fig. 7b)	0.23
E.S.D.U. (z_o = 0.07)	0.23

with E.S.D.U. data for the longitudinal length scale $_xL_u$ then a comparison of a sort may be made by reducing all three spectra to a common dimensionless form as shown in Fig. 5. This shows that both wind tunnel spectra are similarly deficient at the low frequency end compared with the E.S.D.U. standard spectrum. The full-scale spectrum, on the other hand, is slightly biassed towards the low frequency end. In making this comparison it should be acknowledged of course that a scatter of $\pm$ 30 per cent exists normally in data of this type (E.S.D.U. 1974).

6. MEASUREMENTS OF MEAN PRESSURE COEFFICIENTS

Data published from the full-scale tests by the Building Research Establishment include mean pressures measured during two gales in which the mean wind direction was approximately 235°. These runs were designated A7 and A32 by Eaton and Mayne (1975). The wind tunnel measurements described in this section refer to a turntable angular position corresponding to this wind direction (See Fig. 3).

In planning these measurements consideration was given to the significance of the nominally steady and undisturbed reference pressure used in the full-scale experiments. In relation to mean value measurements of course, any unsteadiness is of no significance, but it was felt that the tunnel tests should include a check to see whether or not the mean pressure at the reference point could be affected by the proximity of the buildings.

An equal source of anxiety was the unknown effect upon the tunnel measurements themselves of static pressure gradients; either produced inadvertently in the simulated wind flow over the empty turntable area or produced properly by the model but wrongly exaggerated by blockage effects. These considerations were thought to be particularly relevant in view of the relatively large area of the present site.

Initially, an attempt was made to set up a completely independent, stabilised reference pressure source. This was constructed using a rigid vessel of large thermal capacity, heavily insulated and connected to a pressure tapping far from the model via a very small orifice designed to give a long time-constant of a minute or more. The attempt was abandoned however, when it was discovered that pressure transducers using the stabilized backing pressure were responding to pressure fluctuations arising not from the tunnel flow but from the wind around the outside of the laboratory building.

It was then decided to revert to a system of measurement which was, at least in principle, the same as that used for the full-scale experiments. The transducer backing pressure was provided from a flush pressure tapping at the estate reference position, while the time-constant of the microphone

cavity itself was relied upon to produce a reasonable damped reference pressure characteristic.

In the wind tunnel experiments, as in the B.R.E. full-scale tests, the reference dynamic pressure used to form pressure coefficients was that associated with the mean wind speed at 10 m above ground level. In the tunnel this pressure was measured directly using a small pitot-static tube mounted at a height of 133 mm over the anemometer mast site near the test house.

As an additional reference, a second pitot-static tube was mounted above the first to monitor the dynamic pressure at 0.4 m (30 m full-scale). This provided a valuable check on occasions when the 10 m (133 mm) flow was thought to have been influenced by local disturbances.

In mounting and connecting the DISA pressure transducer and the scanivalve for these measurements, careful precautions against zero drift due to both temperature fluctuations and vibrations were taken as described in section 2 above. With the estate reference pressure connected directly as a backing pressure to the special port on the transducer body, the front face of the diaphragm was connected by means of a special sealed adapter and a short flexible tube (for vibration insulation) to the common part of the scanivalve.

To provide a positive record of the zero drift, albeit at the cost of doubling the tunnel running time, all 24 of the even-numbered scanivalve ports were connected by a manifold to the backing pressure line. After connecting the estate reference pressure formally to hole 1 and the 10 m and 30 m pitot and static pressures respectively to holes 3, 5, 7 and 9 this left only 19 odd-numbered holes available for actual pressure measurements.

The transducer calibration factor of approximately 160 Nm^{-2} per Volt was checked periodically against a Betz micromanometer and was used as input data for a pressure scanning programme written for the PDP 11 computer.

When initiated, this programme controlled the sequential port selection

on the scanivalve, repeated at each port a pressure measurement sequence and finally returned a printed output list of pressure coefficients together with intermediate data for checking pressures.

The sampling sequence at each of the 48 scanivalve positions consisted of the accumulation at 3.1 ms intervals, of 32768 instantaneous pressure samples to complete a 128 point probability density distribution. The sampling time for this operation was 101.58 seconds. The total sample count was the same as that reported by Eaton and Mayne (1975) for the full-scale experiments. The full scale sampling frequency was 1/32 Hz and the present value was chosen to correspond to this frequency as closely as possible on average, taking account of the differing wind speeds found in the various full-scale experiments.

The uncorrected pressure p_n was then computed from the first probability moment in the normal way. Variance and quantile values were also produced but these are ignored in the present discussion.

To correct the recorded pressures for zero-drift, it was assumed that the appropriate zero reading for the n^{th} pressure must lie between the recorded even-port zero readings p_{n-1} and p_{n+1} taken immediately before and after p_n.* The nominally corrected pressure P_n was then defined by

$$P_n = p_n - \tfrac{1}{2}(p_{n+1} + p_{n-1}).$$

The uncertainty in the zero value used for this nominal correction is such that the worst possible error is ΔP_n where

$$\Delta P_n = \pm \tfrac{1}{2}(p_{n+1} - p_{n-1}).$$

Applying the same procedure to produce a nominally corrected pitot pressure P_3 and static pressure P_5 it may be shown that after calculating the nominally corrected mean pressure coefficient C_{p_n} where

$$C_{p_n} = P_n/(P_3 - P_5)$$

the worst possible error is given approximately by

$$\frac{\Delta C_{p_n}}{C_{p_n}} = \tfrac{1}{2} \frac{|p_{n+1} - p_{n-1}|}{p_n} \cdot \frac{|p_4 - p_2 + p_6 - p_4|}{P_3 - P_5}$$

* This implies the assumption that the zero-drift is monotonic with time.

Thus by examining the computer listing of even-port zero values it was possible to assess the consequences of the unavoidable zero drift rates upon the nominally corrected pressure coefficient for any selected odd port. In the worst case found in the present records the uncertainty appears to be no more than 0.06%. Therefore the nominal drift-correction procedure outlined above was accepted as being more than sufficiently accurate for the present purposes.

A far more significant source of variability in the results was the inevitable consequence of rather short sampling times producing the effect of non-stationarity. This was checked by repeating each run three times and examining the results for evidence of non-random overall trends (e.g. on the average for all values in the set). In the absence of such trends, the three readings were averaged to yield a best estimate of the mean pressure coefficient at each point on the model.

When the standard deviation was checked for each trio of pressure coefficients, deviations were found for which the average over all points on the model was only 2.2 per cent with excursions above 4.5 percent in only four cases, and a single highest deviation of 5.1 per cent.

Pressure coefficients were determined in this way for a total of 44 points on the seven estate houses identified in Fig. 2, and also at 77 points on the test house. The pressure tappings were positioned according to dimensions supplied by the Building Research Establishment with the general arrangement and label code shown in Fig. 9.

Because of the limited scanivalve capacity already explained, the 121 pressure connections were divided into seven sets, with occasional tappings included in several sets as an additional repeatibility check.

The results of this procedure are displayed in Table 2 and 3. Further subsidiary measurements were also made but these are best described in the context of the discussion which follows.

7. DISCUSSION

As the results of relevant wind tunnel investigations accumulate, critical comments on the experiment as a whole will of course become better informed. With the Bristol results (Bray 1977) available as well as the B.R.E. full scale data, the present authors have an advantage in this respect over Bray himself.

7.1 Data Tabulation

Table 2a incorporates the Bristol results as well as the B.R.E. data of Eaton and Mayne (1975) in order to provide an easy comparison. There are no Bristol measurements on the test house (Table 3).

Because both the B.R.E. pressure coefficients and the present results are derived from pressure difference relative to the estate reference point (see Fig. 2), the Bristol pressure coefficients have been adjusted here to the same datum by subtracting Bray's reference hole pressure coefficient of 0.15 from each of his other values.

It is somewhat disappointing to observe, on a superficial reading of Table 2a that while the two sets of wind tunnel data show sporadic evidence of agreement, there is very little sign of direct agreement with the full scale results, which show much higher pressures in general.

7.2 Questions concerning the choice of pressure datum

In discussing this discrepancy, Bray (1977) expressed concern over the possibility of a "bias" in the pressure at the estate reference hole. Regarding this pressure as unreliable he chose to present his pressures relative to a datum measurement at 10 m (full scale equivalent) at the anemometer mast site. Unaccountably however, he failed to convert the B.R.E. coefficients to the corresponding datum before making his comparison.

In Table 2b this has been done. The three sets of pressure coefficients are shown relative to the 10 m static pressure as datum. This is produced from Table 2a simply by adding 0.11 and 0.15 respectively to the Oxford and Bristol coefficients, while the full-scale values are adjusted by subtracting

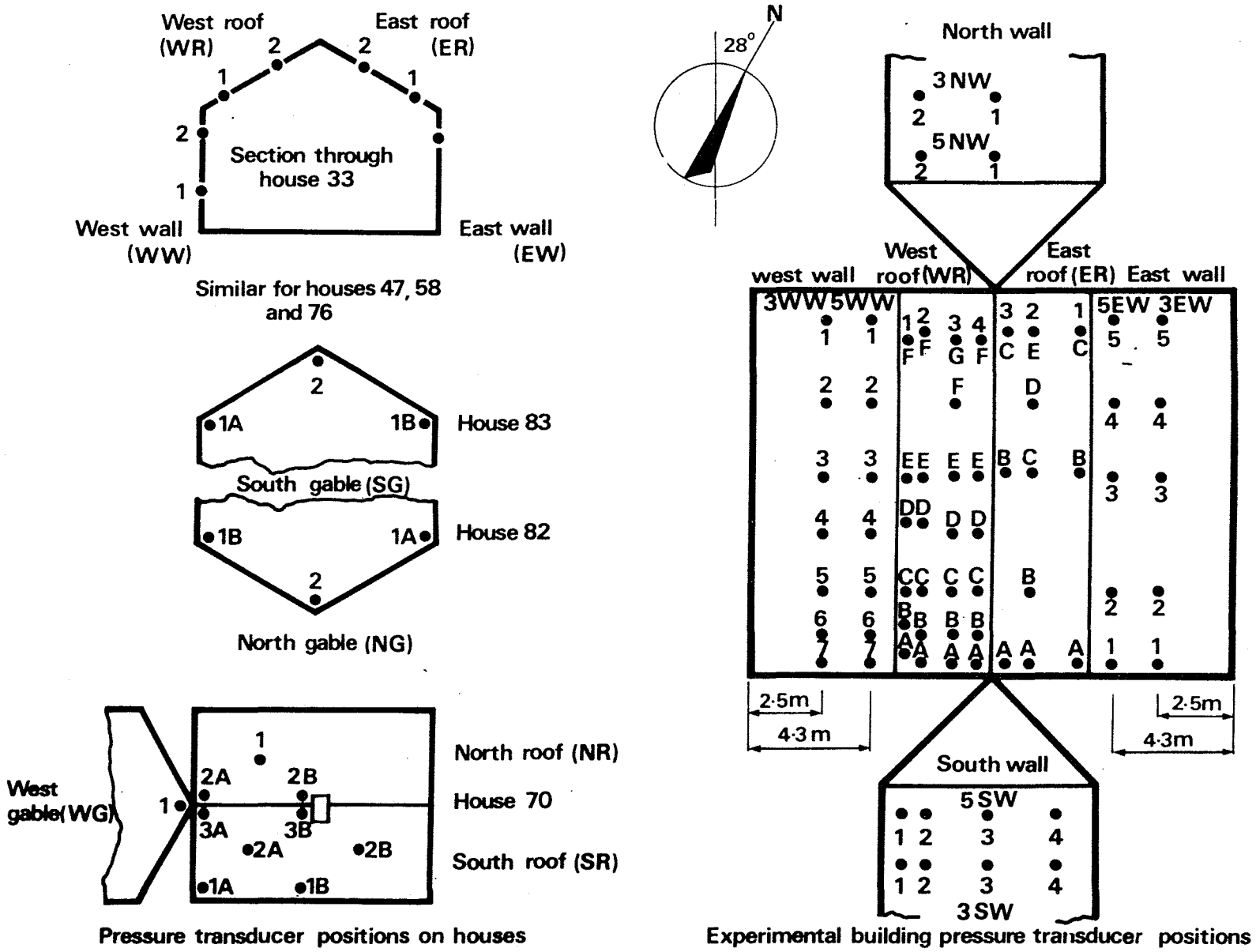

Figure 9 Position of pressure transducers on houses in the estate and on the experimental building

TABLE 2

COMPARISON OF MEAN PRESSURE COEFFICIENTS ON ESTATE HOUSES

WIND DIRECTION $\theta = 265°$ 10 m REFERENCE VELOCITY

POSITION CODE (FIG 9)	A MANHOLE STATIC REFERENCE			B 10 m STATIC REFERENCE		
	B.R.E. A7	OXFORD	BRISTOL	B.R.E. A7	OXFORD	BRISTOL
33EW1	−·12	−·47	−·33	−·20	−·36	−·18
33ER1	+·13	−·67	−·43	+·05	−·55	−·28
33ER2	−·03	−·68	−·45	−·11	−·57	−·30
33WR2	−·07	−·28	−·35	−·15	−·17	−·20
33WR1	+·24	−·24	+·05	+·16	−·13	+·20
33WW2	+·21	−·15	0·00	+·13	−·04	+·15
33WW1	+·24	−·16	−·05	+·16	−·05	+·10
47EW1	−·10	−·42	−·30	−·18	−·31	−·15
47ER1	−·13	−·59	−·45	−·21	−·48	−·30
47ER2	−·12	−·60	−·45	−·20	−·48	−·30
47WR2	+·07	−·29	−·35	−·01	−·18	−·20
47WR1	+·08	−·31	−·15	·00	−·20	0.00
47WW2	+·15	−·08	0·00	+·07	+·03	+·15
47WW1	+·09	−·12	−·05	+·01	−·01	+·10
58EW1	+·09	−·31	−·30	+·01	−·19	−·15
58ER1	0·00	−·44	−·40	−·08	−·33	−·25
58ER2	−·14	−·50	−·45	−·22	−·39	−·30
58WR2	+·19	−·28	−·35	+·11	−·16	−·20
58WR1	+·10	−·29	−·35	+·02	−·17	−·20
58WW2	−·01	−·39	−·43	−·09	−·27	−·28
58WW1	+·15	−·40	−·40	+·07	−·28	−·25
70SR2A	−·36	−·79	−·75	−·44	−·67	−·60
70NR1	−·23	−·87	−·71	−·31	−·75	−·56
70SR1A	−·50	−1·28	−·97	−·58	−1·17	−·82
70SR3A	−·54	−1·13	−1·01	−·62	−1·01	−·86
70NR2A	—	−1.08	—	—	−·97	—
70SR2B	+·43	−·37	−·63	+·35	−·26	−·48
70SR1B	−·23	−·46	−·67	−·31	−·35	−·52
70SR3B	+·07	−·49	−·15	−·01	−·38	0·00
70NR2B	—	−·58	—	—	−·46	—
70WB1	+·30	+·42	+·13	+·72	+·53	+·28
76EW1	−·13	−·48	−·50	−·21	−·37	−·35
76ER1	−·07	−·58	−·50	−·15	−·47	−·35
76ER2	+·02	−·58	−·23	−·06	−·47	−·38
76WR2	−·06	−·30	−·33	−·14	−·19	−·18
76WR1	—	−·52	—	—	−·40	—
76WW2	+·54	+·20	+·05	+·46	+·31	+·20
76WW1	—	+·12	—	—	+·24	—
82NG1A	−·05	−·57	−·55	−·13	−·46	−·40
82NG2	−·03	−·61	−·60	−·11	−·49	−·45
82NG1B	+·07	−·77	−·75	−·01	−·66	−·60
83SG1B	−·13	−·64	−·65	−·21	−·52	−·50
83SG2	−·31	−·64	−·65	−·39	−·53	−·50
83SG1A	−·59	−·92	−·95	−·67	−·80	−·80
MANHOLE	DATUM	DATUM	DATUM	−·08	+·11	+·15
10m PITOT	—	+·89	—	—	+1·00	—
10m STATIC	+·08	−·11	−·15	DATUM	DATUM	DATUM
30m PITOT	—	+1·31	—	—	+1.42	—
30m STATIC	—	−·16	—	—	−·05	—

TABLE 3

COMPARISON OF MEAN PRESSURE COEFFICIENTS ON TEST HOUSE

WIND DIRECTION $\theta = 265°$ ROOF ANGLE $22\frac{1}{2}°$

POSITION CODE (Fig 9)	WALL PRESSURES			POSITION CODE (Fig 9)	ROOF PRESSURES		
	B.R.E. A7	B.R.E. A32	OXFORD		B.R.E. A7	B.R.E. A32	OXFORD
3WW 1	—	+·09	+·22	WR 1A	-·13	-·20	-·60
3WW 2	—	+·21	+·40	WR 1B	—	-·34	-·66
3WW 3	+·24	+·29	+·44	WR 1C	—	-·20	-·66
3WW 4	+·26	+·29	+·45	WR 1D	—	-·22	-·65
3WW 5	+·21	+·29	+·47	WR 1E	-·19	-·26	-·67
3WW 6	+·06	—	+·40	WR 1F	—	-·42	-·67
3WW 7	-·09	—	+·25				
				WR 2A	—	—	-·18
5WW 1	—	+·34	+·37	WR 2B	—	—	-·23
5WW 2	—	+·51	+·50	WR 2C	—	—	-·40
5WW 3	-·27	+·50	+·53	WR 2D	—	—	-·43
5WW 4	—	+·54	+·54	WR 2E	—	—	-·47
5WW 5	—	+·51	+·55	WR 2F	—	—	-·37
5WW 6	—	+·46	+·55				
5WW 7	-·12	+·35	+·31	WR 3A	+·21	-·10	-·10
				WR 3B	+·28	-·03	-·11
3EW 1	-·48	-·43	-·33	WR 3C	+·24	+·02	-·13
3EW 2	—	-·48	-·36	WR 3D	—	-·08	-·17
3EW 3	-·46	-·47	-·32	WR 3E	+·46	—	-·16
3EW 4	—	-·54	-·33	WR 3F	—	—	-·19
3EW 5	—	-·53	-·37	WR 3G	—	—	-·22
5EW 1	-·51	-·37	-·34	WR 4A	+·02	-·05	-·27
5EW 2	—	-·39	-·35	WR 4B	—	—	-·27
5EW 3	—	-·42	-·33	WR 4C	—	—	-·30
5EW 4	—	-·47	-·35	WR 4D	—	—	-·30
5EW 5	—	-·52	-·39	WR 4E	+·01	-·12	-·32
				WR 4F	—	—	-·32
3SW 1	-·58	-·49	-·76				
3SW 2	-·70	-·73	-·63	ER 1A	+·19	-·56	-·41
3SW 3	-·60	-·51	-·39	ER 1B	-·50	-·63	-·45
3SW 4	-·49	-·28	-·27	ER 1C	—	-·58	-·47
5SW 1	—	-·78	-·65	ER 2A	-·26	+·20	-·43
5SW 2	—	-·74	-·66	ER 2B	—	-·38	-·41
5SW 3	—	—	-·34	ER 2C	—	—	-·40
5SW 4	—	—	-·27	ER 2D	—	—	-·41
				ER 2E	—	—	-·44
3NW 1	+·06	-·66	-·57				
3NW 2	-·56	-·76	-·61	ER 3A	-·06	-·16	-·41
				ER 3B	—	—	-·38
5NW 1	—	—	-·58	ER 3C	—	—	-·44
5NW 2	—	—	-·66				
				OH - U			
				OH - L			
MAN HOLE	DATUM	DATUM	DATUM				
10m PITOT	—	—	+·88				
10m STATIC	—	—	-·12				
30m PITOT	—	—	+1·30				
30m STATIC	—	—	-·16				

0.08 (Eaton and Mayne 1975). Table 2b then shows these corrections as non-zero values of the estate reference pressure.

It was the opposite sign of the Bristol and Full-Scale values of this reference pressure which provoked Bray's original comment. With the addition now of the Oxford Measurements it would appear that his suspicions have some justification. Certainly when the estate reference pressure datum is discarded in favour of the 10 m static pressure as in Table 2b the correlation between the two sets of wind tunnel data is not harmed, while the agreement with the full scale results shows a definite improvement.

7.3 Relevance of pressure datum

In making such a comment it must be acknowledged that its relevance is to questions of experimental technique only. To the structural engineer the choice of a pressure reference is of no consequence whatsoever. His concern is merely to know about the variation of pressure over the surface of a particular building- or probably more often between an external surface and an internal surface.

In relation to tests like the present one, involving several buildings or an extensive site, but with a single pressure datum, it becomes even more important to acknowledge this distinction. By doing so it is possible to maintain a proper perspective in discussing discrepancies between different sets of experimental results.

7.4 Modified comparison of pressure distributions

With this in mind, a diagrammatic presentation is given in Fig. 10 of the tappings in the straight line of houses designated 76, 58, 47 and 33 in Fig. 2. Ignoring any length scale, the four sets of seven pressures are laid out in order as they appear in an approximately down-wind traverse across the estate.

The data plotted is from Table 2a. Because of the choice of datum the overall pressure levels differ as already noted. However, provided that this difference in level is ignored, the diagrammatic presentation

reveals that there are in fact some encouraging similarities between the shapes of the three sets of pressure distributions.

7.5 Comments on discrepancies and similarities

Without distinguishing very clearly between the shape and the level, Bray (1977) in his detailed comparison felt that the full-scale values at holes 58WW2 and 33ER1 did not fit very well into his pattern. Ignoring the levels, and with the pattern reinforced by the addition of the Oxford results in Fig. 10, the comment might be made that it is point 58WW1 rather than 58WW2 (full scale) which does not fit the pattern while 33ER1 would look better with a change of sign. Also, since there is a fairly strong indication that pairs of holes on the same surface should experience fairly similar pressures, then perhaps Bray's own value at 47WR2 might possibly be queried.

Queries relating to individual data points are of course rather invidious. The profit in this exercise arises rather from the way in which it demonstrates by implication that there is a pattern of similarities which can be observed and against which the discrepancies stand out.

7.6 Varying scale of pressure distrubution

If these similarities are accepted, then it is instructive to make a closer examination of the characteristics of the pressure distributions on the four individual houses.

A feature which is apparent immediately in Fig. 10 is that the scale of the pressure variation differs from house-to-house. After an obviously strong pattern over the windward house (76) the scale becomes relatively small in house 58 which is separated from 76 by only 28.5m, and is obviously sheltered. On the succeeding houses 47 and 33 however the magnitude of the pressure variation increases slightly despite the fact that these houses lie deeper in the estate.

7.7 A tentative explanation

A possible explanation of this increase is that the windward rows

FIG 10

COMPARISON OF ESTATE HOUSE PRESSURE DISTRIBUTIONS (FROM TABLE 2A)

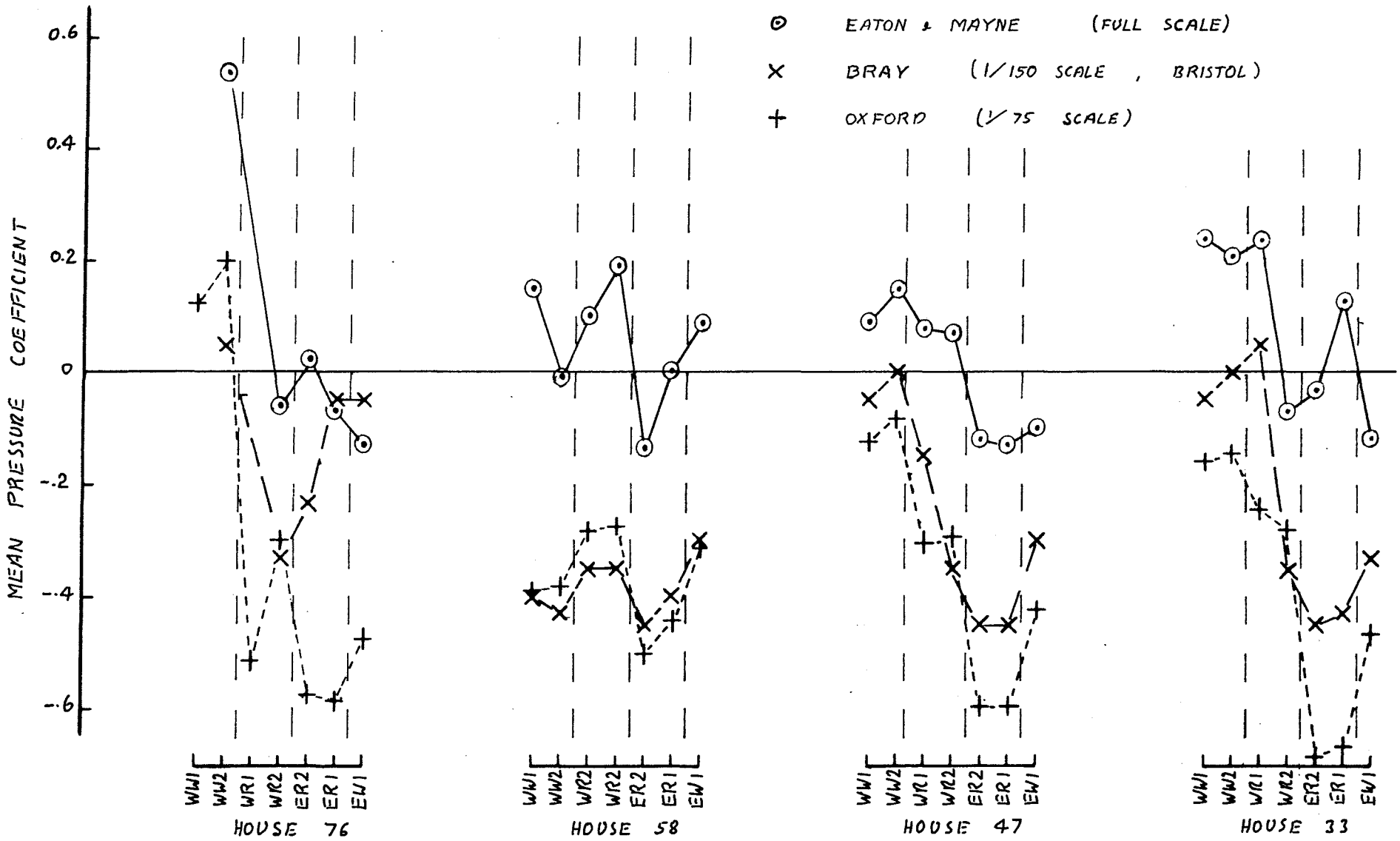

of houses cause additional turbulent mixing which effectively increases the wind speed over the downstream rows, thus eventually overcoming the shelter effect which is apparent on the second row.

7.8 Smoke visualisation

Some rather subjective confirmation of this idea was obtained by studying a video recording of some smoke visualisation tests. This showed a fairly extensive region of separated flow shielding the second row of houses. Although unsteady, this region was fairly clearly defined on average and was bounded by a mean dividing streamline extending from the roof apex of the windward row to somewhere near the upstream roof face of the second row. The existence of this clearly defined region explains why the upstream wall pressures on this particular house are actually lower than the upstream roof pressures. House 58 appears to be unique in this respect (see Fig 10.)

Although local flow separation could be observed intermittently at the roof apex of each succeeding row of houses, the separated flow regions were quickly dominated by the arrival of strong eddies from upstream and were thus not clearly in evidence behind any row other than the first.

7.9 Local velocity measurements

In order to obtain further quantitative evidence relating to this hypothesis, measurements were made of the mean velocity and the turbulence intensity at similar points 90 mm (6.75 m) upstream of the windward wall and 133 mm (10 m) high in the plane of the pressure tappings for each of the four houses. The traverse height was chosen after using the probability density display facility of the velocity profile programme, described in section 5 above, to detect the occurrence of significant flow reversals which would have corrupted the hot-wire anemometer record and spoiled the mean velocity computation.

The values obtained in this survey are shown in Table 4

TABLE 4

Local velocity measurement upstream of individual estate house rows

House	Mean Velocity	Turbulence intensity
76	4.59	0.24
58	4.28	0.33
47	3.71	0.40
33	4.30	0.34
Mast Site	5.12	0.21

While these figures confirm the greatly increased level of turbulence caused by the upstream houses, they do not show (at least at the measurement height which is well above the 6.75 m rooftop level) any variation in mean velocity which is consistent with the indications on the pressure distributions of Fig. 10. Unfortunately the direction ambiguity characteristics of hot-wire anemometers made it pointless to attempt measurements at a lower level.

7.10 Tunnel Pressure Gradients

In the preceding discussion, it has been recognised that the absolute values of pressure coefficients recorded in any test are irrelevant to the user of wind loading data. However, inasmuch as the present comparison of results is also important as a test of experimental techniques, it is profitable to add some comments upon the problem of the observed disparities in pressure datum levels.

Considering the factors which may have a bearing upon this problem, there are two fairly obvious ways in which wind tunnel flows may contain pressure fields which differ from those found in full-scale natural wind flows. These are spurious pressure gradients and blockage effects which may distort correctly generated pressure fields.

Streamwise pressure gradients, arising perhaps from the growth of wall boundary layers, exist in many conventional wind tunnels. In wind-simulation work where very thick boundary layers are grown deliberately and very rapidly, it is important to ensure that any corresponding pressure gradients are eliminated in order to match the atmospheric pressure field. Here the only pre-existing gradients arise from Coriolis effects and are negligible when compared with disturbance pressures around buildings. For this reason the present Oxford wind tunnel is provided with an adjustable taper facility in the working section. This was not used in the present study, but once the final flow simulation was established (see section 5 above), a check was made on the pressure distribution over the flat surface of the empty turntable. The resulting surface pressure distribution, plotted in Fig. 11 shows a slight negative pressure gradient. Expressed in coefficient form based upon the mean dynamic pressure at 0.133 m (10 m) this corresponds to a gradient of -0.069 per metre in the tunnel or -9.2×10^{-4} per metre at full scale.

This observation has an important bearing upon the discussion initiated by Bray (1977) of the possibility of a "bias" in the full scale reference pressure datum (see above with Tables 2 and b.). In checking this bias, the reference hole pressure has been compared with an alternative measurement of static pressure on the anemometer mast 77 m further upstream. Over this distance, the pressure gradient in the Oxford tunnel corresponds to a pressure coefficient of 0.071. Bray does not report any check on the pressure gradients associated with his 1/150 scale wind simulation in the Bristol tunnel. However, it is clear that gradients of order 10^{-3} (full scale) are quite possible and that they are not insignificant when discussing small pressure differences giving coefficients of -0.08 (B.R.E.), + 0.11 (Oxford), +0.15 (Bristol), which are measured over distances as large as 77 m.

Applying the measured Oxford pressure gradient to the reference manhole pressure measurement as a correction yields a bias relative to the anemometer mast pressure of +0.18 instead of 0.11.

7.11 Static pressure errors in using a pitot-static tube

Unfortunately, tunnel pressure gradients are not the only source of error affecting the present discussion. In checking the supposed reference pressure bias, both Bray in Bristol and the present authors in Oxford used a pitot static tube as a convenient device for measuring the static pressure at the mutually agreed secondary reference point at 10 m on the anemometer mast. Both measurements were subject therefore to a source of error which is thoroughly well documented in the literature (e.g. Goldstein 1936, Fage 1936, Toomre 1960), namely the error in apparent static pressure due to transverse turbulence components.

Toomre's asymptotic expressions describe the equal and opposite errors predicted for cylindrical probes which are very small and very large compared with the prevailing turbulence length scales. Using these expressions, Wood (1977) pointed out that a very simple and convenient equation can be written for the difference between the two measurements in terms of the transverse components of the turbulence intensity.

$$\Delta = \frac{\overline{P}_{sm} - \overline{P}_s}{\frac{1}{2}\rho\overline{V}^2} = 2\left\{\left(\frac{\sigma_v}{\overline{V}}\right)^2 + \left(\frac{\sigma_w}{\overline{V}}\right)^2\right\}$$

The dimensionless pressure coefficient error Δ can be evaluated very conveniently using data for the horizontal and vertical turbulence intensities $\sigma_v/\overline{V}$ and $\sigma_w/\overline{V}$ contained in the E.S.D.U. data sheets (E.S.D.U. 1974). Values appropriate to the present simulation (z_o = 0.07) taken at a series of heights are used to obtain the graph shown in Fig. 12.

An experimental indication of the effect of this error was obtained when, in the course of the pressure gradient survey in the Oxford tunnel described above, a pitot-static tube was traversed above the line of surface pressure tappings at a height of 0.4 m (30 m full scale).

The static pressures indicated by the instrument are plotted in Fig. 11. When compared with the straight line drawn through the surface pressure data, the values from the pitot-static tube show a systematic discrepancy, despite the scatter, which corresponds to a pressure coefficient error of 0.047

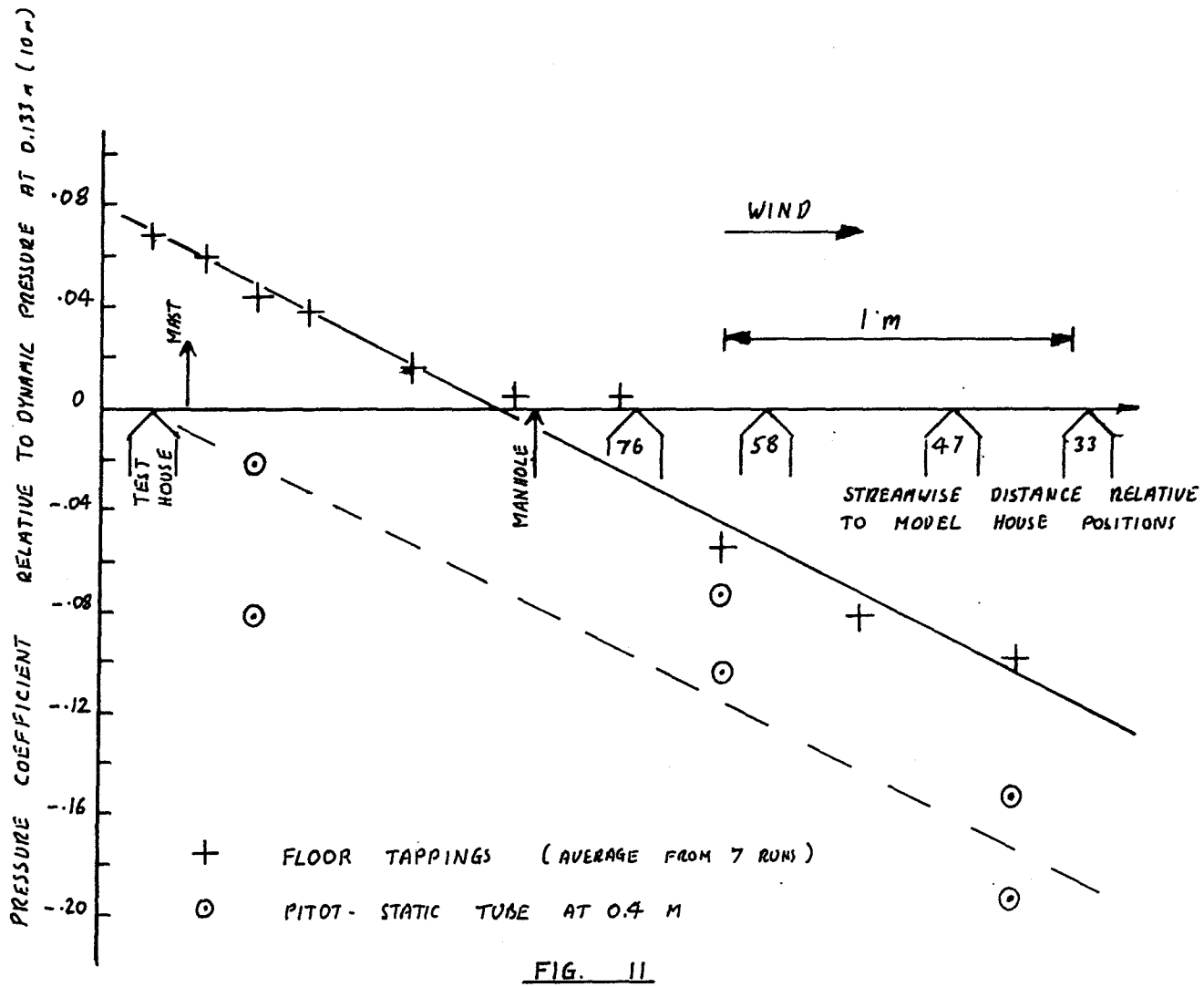

FIG. 11

STATIC PRESSURES ON EMPTY TURNTABLE AND BY PITOT-STATIC TUBE AT 0.4 m (30 m)

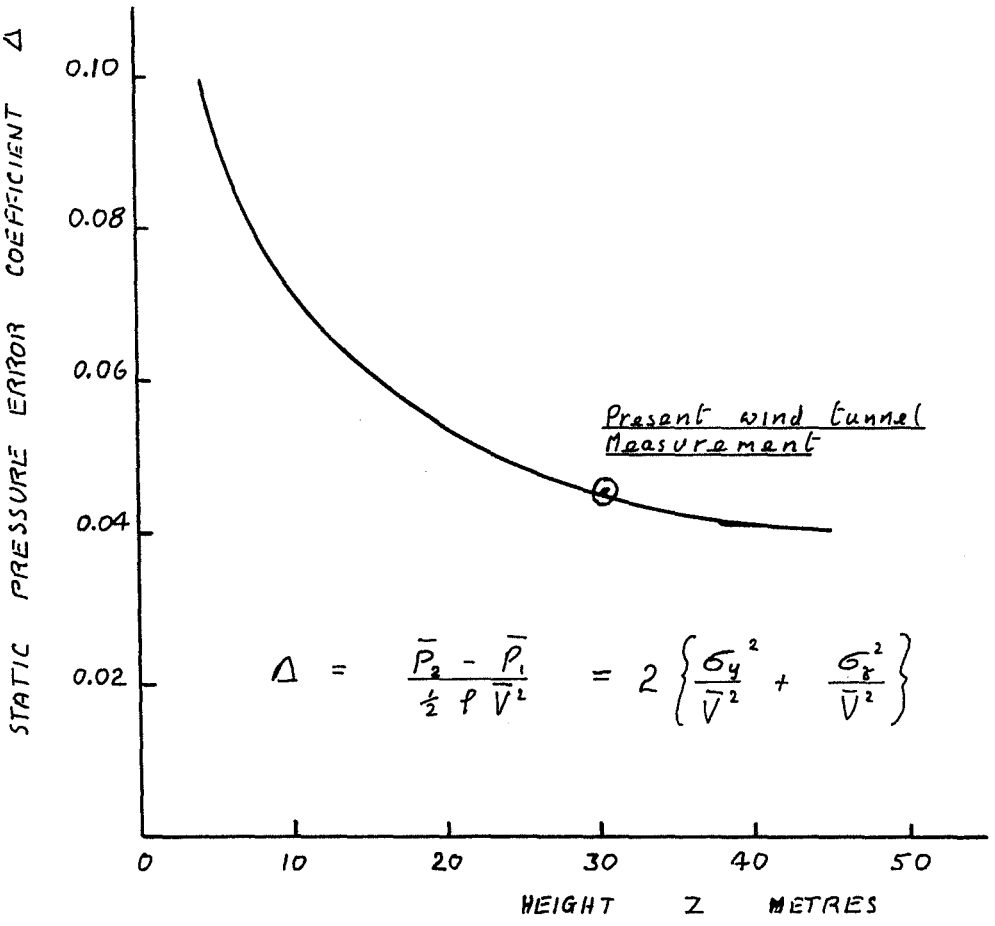

FIG 12

ESTIMATED STATIC TUBE ERROR FOR E.S.D.U TURBULENCE INTENSITIES WHEN $Z_o = 0.07$ m (AFTER TOOMRE 1950)

If it is assumed that the pressure $\overline{P}_2$ recorded by a very large static pressure probe is the same as that observed on a flat wall, then a direct comparison may be made with the value 0.046 given for Δ by the above equation (Figure 12). While the excellent agreement is perhaps a coincidence, nevertheless there remains a fairly convincing demonstration that a significant discrepancy exists. Toom e's theory suggests that the time static pressure lies above the probe value and below the wall value.

7.12 Correction of datum pressure estimates

If this error, taken to be 0.047, is corrected in addition to the compensation already applied for the tunnel pressure gradient, then the present estimate of the estate reference manhole pressure relative to the secondary reference on the anemometer mast reduces again from +0.18 to +0.13.

By making some further tentative and rather arbitrary assumptions it is now possible to pursue fully the consequences of these corrections in relation to Bray's suspicion of an error in the full scale reference pressure.

Eaton and Mayne (1975) used a Marshall probe to measure the secondary static pressure reference on the full-scale anemometer mast. Assuming that this reads correctly so that the only remaining source of error is the reference pressure manhole itself, then the final difference between the corrected Oxford estimate of the manhole pressure (+0.13) and that found by Eaton and Mayne (-0.08) is 0.21. If the full scale pressure distribution in Fig. 10 were to be displaced by this amount then the agreement with the wind tunnel results would become very much closer.

However, in view of the discovery of a pressure gradient, at least in the Oxford tunnel, it is now no longer sufficient simply to apply a constant correction. It is also necessary to adjust the wind tunnel pressure coefficient at every point so that each describes the difference not from a constant reference but from the undisturbed pressure value relevant to that point. As a compromise the average correction deduced from Fig. 11

for each individual house is shown in Table 5.

7.13 Comparison of corrected estate pressures

In Fig. 13, both the constant reference pressure adjustment and the pressure gradient correction have been applied to the pressure distribution originally displayed in Fig. 10. The improvement in agreement is quite gratifying but it should be emphasised once more that the purpose of this examination is not so much to eliminate discrepancies as to offer plausible explanations for them and to demonstrate the relative significance of a few likely sources of experimental error. If the object had been merely to produce data acceptable to the structural engineer, then in the opinion of the authors it would have been equally valid to ignore every one of the errors so far discussed and merely to shift the various house pressure distributions to match, say, the mean values over each group of tappings.

TABLE 5

Pressure Gradient Corrections for Oxford Pressure Coefficients

House	Add to Table 1 Pressure Coefficient
33	+0.127
47	+0.100
58	+0.054
76, 70, 82/3	+0.027
Manhole	+0.005 (nominal datum)
Test house	-0.068

FIG 13

ESTATE HOUSE PRESSURE DISTRIBUTIONS (EFFECT OF DATUM ADJUSTMENTS)

SEE ALSO FIG 10

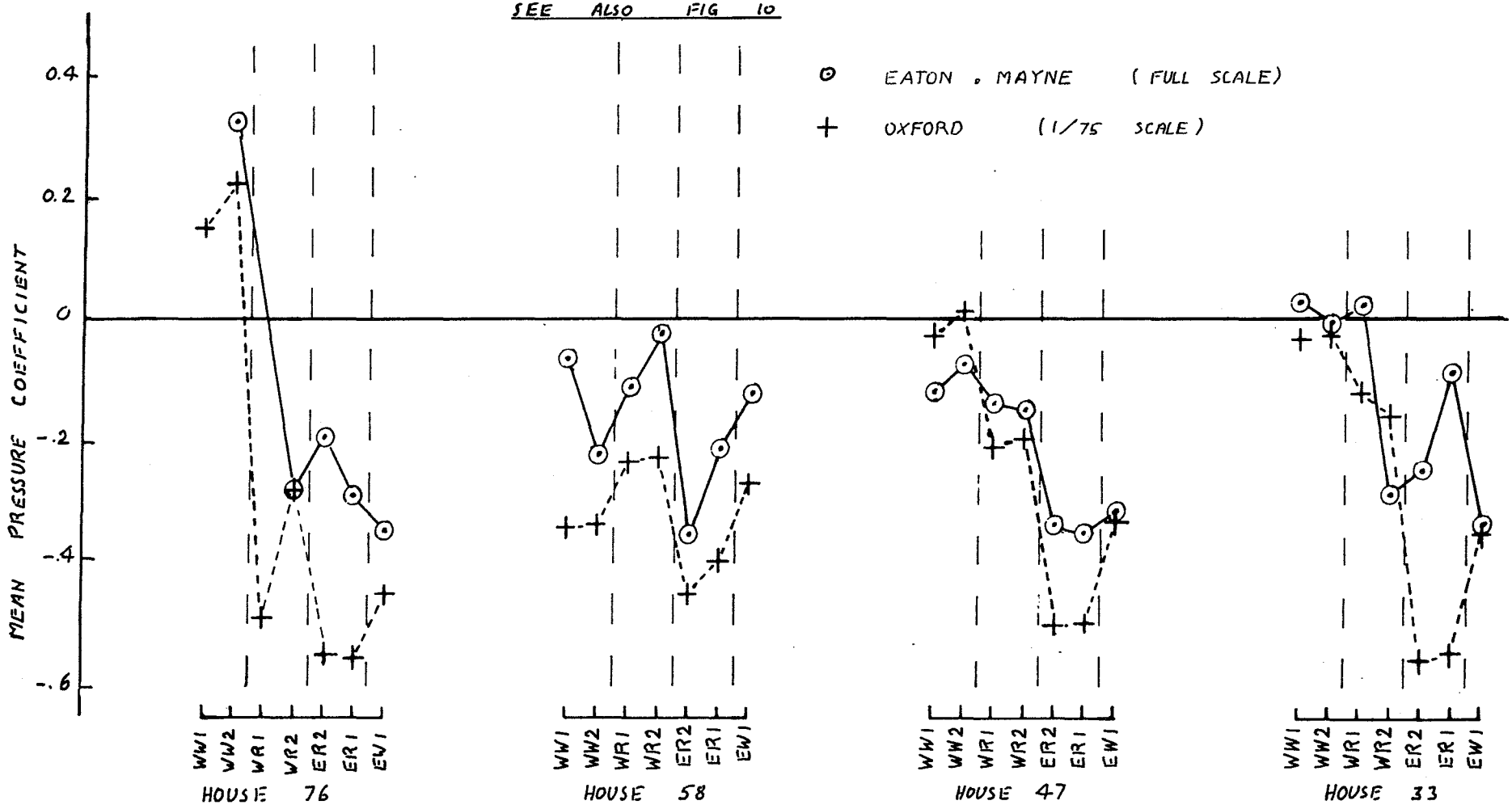

7.14 Upstream Influence of Estate Houses on ground surface pressures

One further comment may be of interest in relation to the choice of a pressure reference site. In positioning the reference pressure manhole some 18m to the west (upstream in the present discussion) of the westernmost row of estate houses, and in an open area, Eaton and Mayne (1975) clearly hoped that the presure at this point would not be affected by the presence of the houses.

Because of the limited relevant area available for surface pressure tappings, it was not possible to perform the obvious wind tunnel check on this assumption by comparing surface pressures with and without the model. Instead, after completing the empty tunnel pressure gradient survey described above, a single strip of wood 73 mm wide, 34 mm high and approximately 1.5 m long was laid on the otherwise empty turntable across the existing line of pressure tappings and at right angles to the flow direction.

Repeating the previous pressure survey with this obstruction, and also with a double-sized one made by stacking four identical bars, yielded the pressure distributions shown in Fig. 14a. The three distributions intersect in the graph, at the pressure hole used as a transducer reference. From this, the more instructive form of Fig. 14b was traced by adjusting all three curves to a common asymptote as far upstream as possible. The correctness of this procedure is confirmed by the fact that the two disturbance curves then re-approach the empty tunnel pressure distribution far downstream. At the same time, the different block sizes are reflected in the approximate doubling of the extent of the pressure disturbance for the double-sized block.

It is the upstream extent of the pressure disturbance which is of interest in the present discussion. Both blocks were smaller than the 90 mm height of the house models, nevertheless their upstream influence on the ground pressure distribution extends for a distance equivalent to at least 90 m full-scale. Thus, if this effect were reproduced in full-scale, it is to be expected that the reference manhole must have been well within the pressure disturbance area.

In view of this, the result of Eaton and Mayne (1975) showing a manhole pressure lower than that on the reference anemometer mast 77 m further from the estate would be somewhat surprising in a westerly wind, but less so if the wind were from the east. The actual direction of the wind during this measurement was not stated.

7.15 Influence of Test House upon Reference Pressure

Recognising that Bray (1977) had omitted the test house and one or two nearby arboreal details from his model, a rapid check was made of the effect of removing the test house and a large tree. The resulting change in the pressure difference between the anemometer mast site and the reference manhole site was too small to be distinguished from normal statistical fluctuations. The possibility of similar changes at both points was not checked.

7.16 Tunnel Blockage

It had been hoped that the experiment with different block sizes might reveal the presence or otherwise of tunnel blockage effects. A similar obstruction (the traverse gear beam) in the high speed flow near the tunnel roof had been observed during the pressure gradient survey to cause a distinct pressure change on the tunnel flow when moved to a position above the turntable. However, the scatter in the pressure measurements (Fig. 14a) is such that no conclusion could be drawn.

With an area blockage of only 2 per cent, a large effect would not be expected of course and it is reasonable to assume that blockage effects are negligible in the present experiments at least as far as local pressure distributions (as opposed to large-scale gradients) are concerned. However there remains a need for further study of this question in the context of sheared flows where the effect of an obstruction on the low speed side must be different from that of a corresponding blockage on the high speed side.

7.17 Comments on Test House Pressures

As already stated, test house pressures were not measured by Bray (1977)

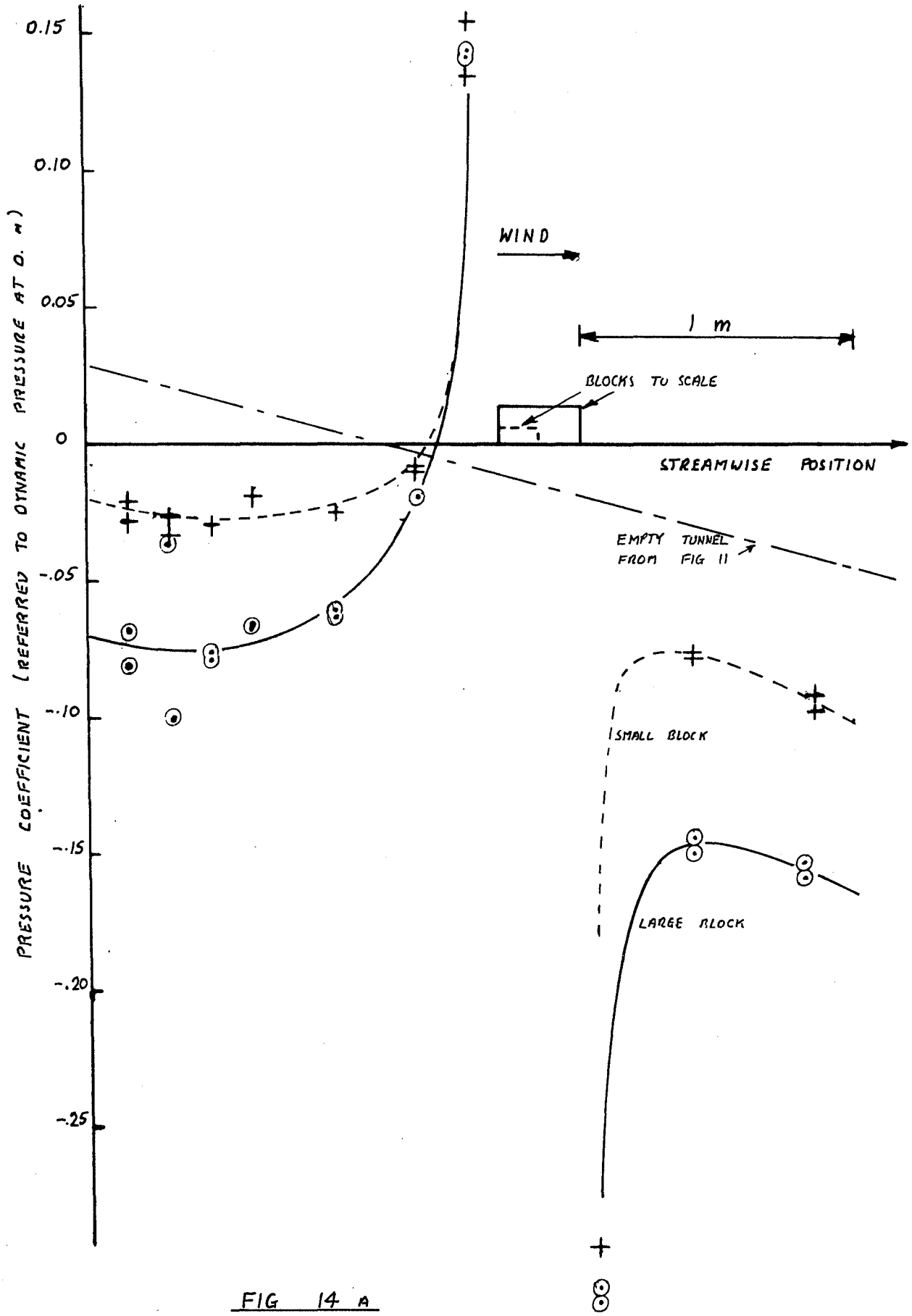

FIG 14 A

TUNNEL FLOOR PRESSURE DISTRIBUTIONS CAUSED BY ISOLATED 2-D RECTANGULAR BLOCKS

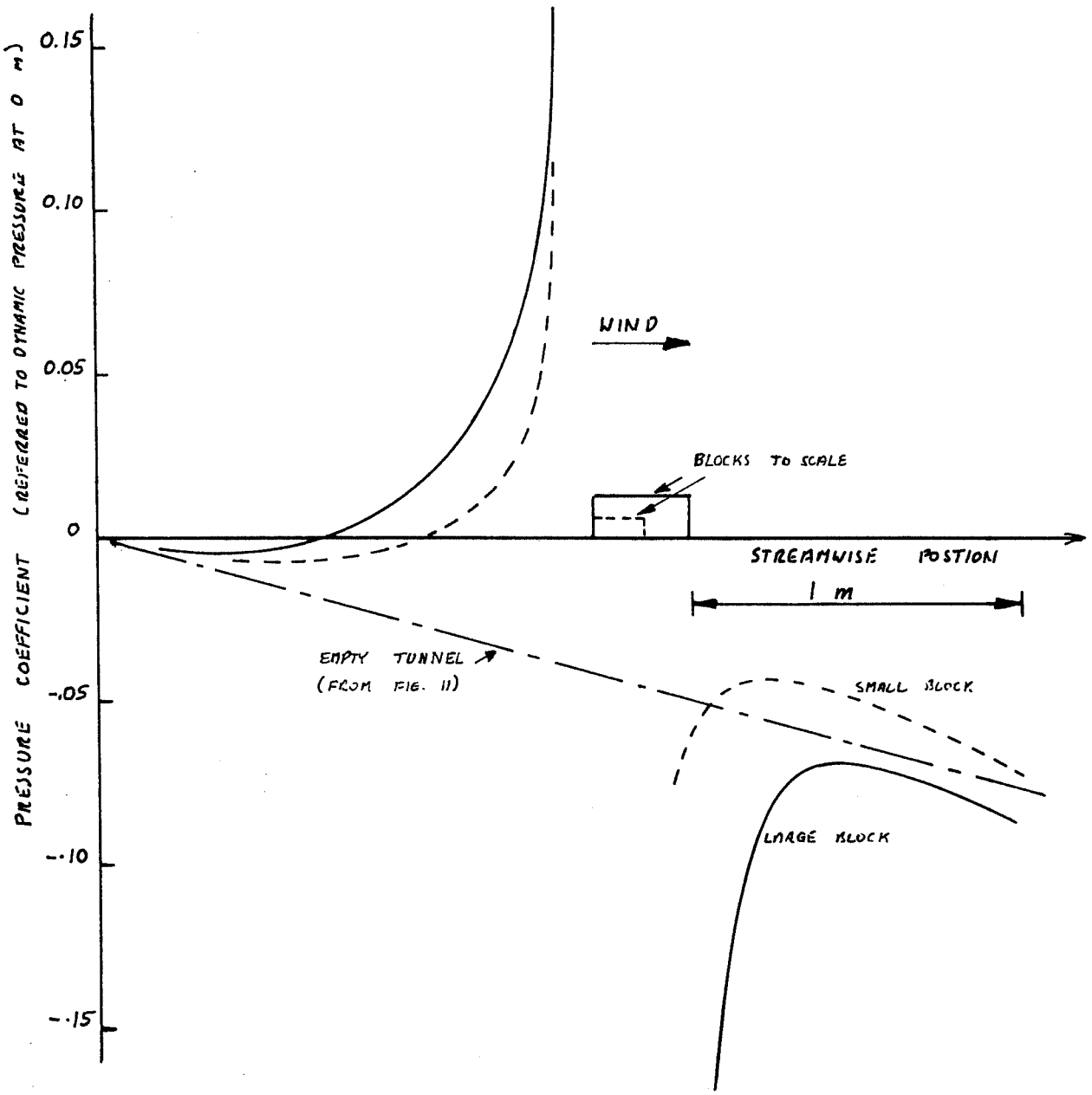

FIG 14 B

DISTURBANCE PRESSURE DISTRIBUTIONS ON TUNNEL FLOOR CAUSED BY 2-D. RECTANGULAR BLOCKS

(TRANSFERRED FROM FIG 14 A)

and at the time of writing, measurements by Cook and by Apperley have not yet been published. Therefore the present discussion is limited to a comparison between the measurements made so far at Oxford, for a single roof angle of 22½ degrees, and the full-scale results of Eaton and Mayne (1975).

A complete comparative list of pressure coefficients is given in Table 3. These are as measured, although Table 5 suggests that the Oxford pressure coefficients might well be reduced by 0.07 to compensate for tunnel pressure gradients etc. as discussed in section 7.10-7.12 above.

In order to relate the present discussion to the previous comparison of estate house pressures, a section pressure distribution, plotted from the data in Table 3, is shown in Fig. 15. Examining this it is clear that the model and full-scale patterns bear a reasonable similarity and that if the wind tunnel results were shifted by -0.07 (Table 5) then the agreement would be very good on both the windward and leeward walls.

On the roof the agreement is poor. The principal feature of the disagreement is the strong suction on the model near the lower edge of the windward face. This produces generally lower roof pressures although the discrepancy does vary on the leeward face.

When investigating possible causes of this high corner suction, various attempts were made to modify the detailed modelling of the gutter but with no apparent effect.

The smoke visualisation tests previously described did not reveal it sufficiently clearly to warrant a positive comment but it is suspected that a small separation bubble on the model may have enveloped the WR1 row of tappings, thus exposing them to the influence of the corner pressure in a way that would not have occurred at full-scale. Certainly it is leading edge corner flows of this type which are likely to cause the greatest difficulty in low Reynolds number experiments where scale effects are ignored. It will be interesting to see whether the results of other

investigations expected soon will shed any light on this question. Unfortunately most of the estate house results are really too sparse and variable to be of any assistance in this matter. The only exception is house 70 which has its gable end facing the wind and some roof pressure tappings very close to the edge. Both Bray (1977) and the present results (Table 2) show extremely low pressures here which again are only partly supported by the full-scale results.

7.18 Gable End Pressures

Prompted no doubt by known instances of the collapse of gable ends under severe wind conditions, the full-scale experiments of Eaton and Mayne (1975) included pressure measurements on the gable ends of houses 82 and 83 as well as on the end walls of the test house. The wind direction recorded during runs A7 and A32, and which is reproduced in the present wind tunnel experiments, is at 265^{o} to the line of the estate. Thus the end walls in question are inclined at 5 degrees to the wind direction (see Fig. 2) in such a way that the test house south wall and the gable of house 83 may be described as windward faces whilst gable 82 and the test house north wall are leeward faces.

Full scale measurements on the test house with $22\frac{1}{2}^{o}$ roof pitch are slightly suspect because the pressure transducers are covered by part of the adjustable gable panel. Nevertheless Table 3 shows reasonable agreement between full-scale and model scale results in showing that pressures are lower on the north wall centreline than at corresponding points on the south wall. Intuitively, this is an entirely reasonable relationship.

Near the west corners the pressures are equalised presumably under the influence of similar corner separation flows.

Making a similar comparison between the gable ends of houses 82 and 83, which face each other across a narrow passage, it is curious to observe from Table 2 that is it now the windward face (83) which experiences the lower pressures. This observation is confirmed in Table 2 by data from all three sources.

FIG. 15

COMPARISON OF TEST HOUSE PRESSURE DISTRIBUTIONS

(DATA FROM TABLE 3)

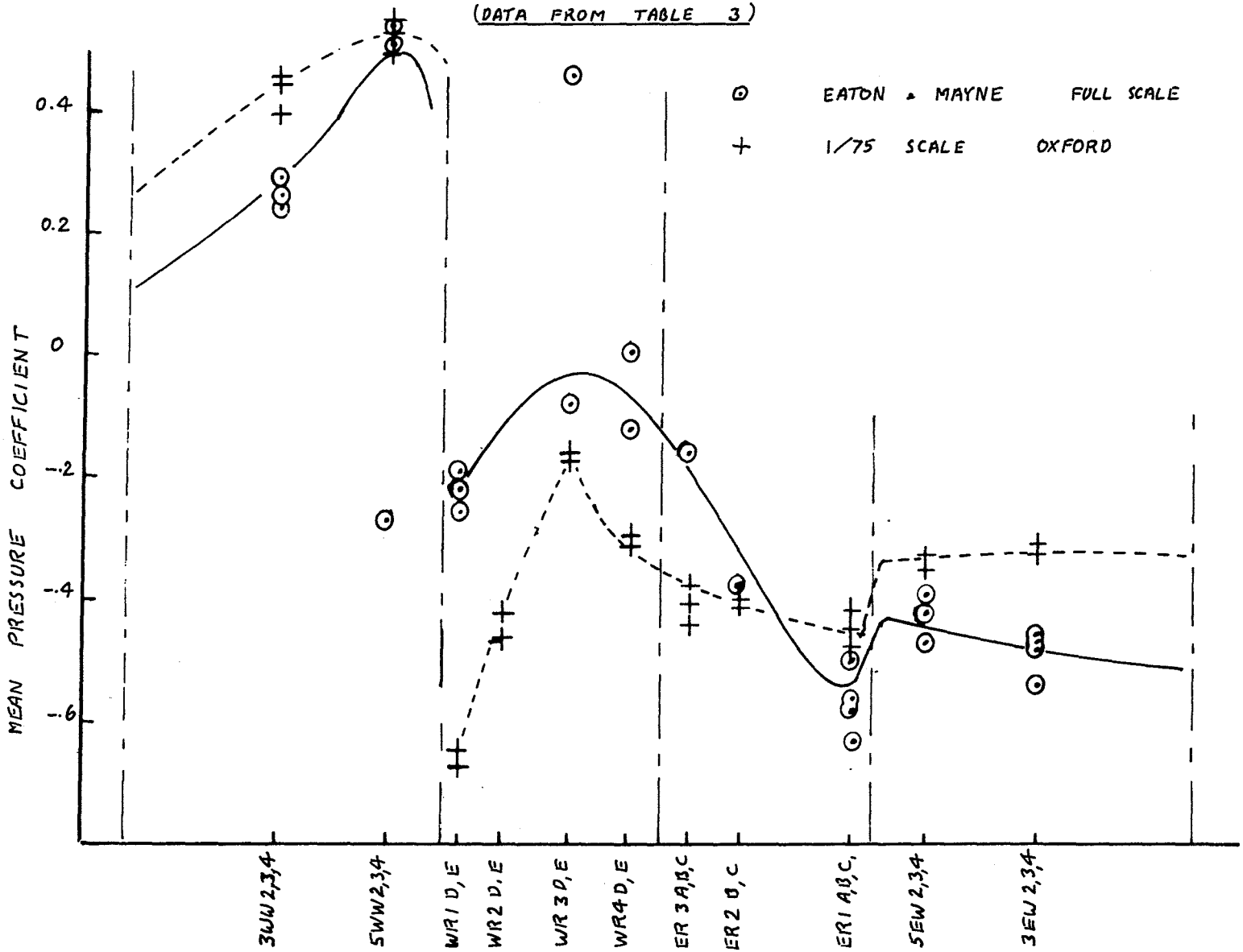

In seeking an explanation for these pressures a brief smoke visualisation experiment was conducted. The flow on the west wall of the test house was found to pass intermittently towards the north end and the south end, with a slight bias as expected towards the north. On house 83 on the other hand, an unusually strong - indeed almost continuous - tendency was observed for the west wall flow to be directed southwards towards the passage. The reason for this flow appears to be the set-back position of house 83 relative to the rest of the row (see Fig. 2), and its effect is apparently to annul the small northward component of the incident air flow.

The pressures on both gables are low and fall towards the downstream corner.

8. CONCLUSIONS

As disclosed at the outset, the scope of the work described in this first report is limited to the development of a single wind simulation and the measurement of mean pressure coefficients for a single wind direction. These particular test conditions were chosen in order to maximise the opportunity for critical assessment in relation to previously published work. Further measurements and related comments are due to appear in subsequent parts of the report.

Taking advantage of the availability, including the present results, of two independent sets of wind tunnel data as well as the full-scale results, it has been possible to recognise many common features in the mean pressure distributions. This permits the present report to focus attention more sharply, and with rather more confidence than before, upon what appears to be a major cause of disparities between mean pressure data from different sources. As suspected by Bray (1977) this is the difficulty in relating a chosen pressure datum level from one experiment to another. The problem is particularly severe on large-area sites like the present one, where not only measurement errors but even small tunnel pressure gradients may cause significant difference between pairs of widely separated points.

Although the significance of this problem is considered in relation to experimental technique, it is also exphasized that the value of the data to the structural engineer is unaffected because he is entirely concerned with fairly local pressure differences rather than absolute values. Thus in commenting upon various features of the measured pressure distributions, it has been possible to consider variations and differences above whilst ignoring differences in datum level. When viewed in this way, agreement between the full-scale results and data from the two wind tunnel investigations is quite encouraging in the majority of cases.

An exception which is worthy of comment is the fairly consistent disagreement near upstream sharp corners. In these regions, wind tunnel

pressures appear to fall more sharply than those measured at full-scale and it is suspected that this is where scale effects are most likely to be troublesome.

9. ACKNOWLEDGEMENTS

The authors wish to express their thanks to Mr. R. Belcher who not only conducted routine experiments with patient care but who also found the energy to respond to sudden ideas by producing new experiments at a moment's notice.

The work described in this report is supported by a grant B/RG/5912.6 for the Science Research Council.

10. REFERENCES

BRAY, C. G. (1977) University of Bristol, Thesis.

COOK, N. J. (1973) Atmos. Environment 7, 691.

COUNIHAN, J. (1969) Atmos. Environment 3, 197.

EATON, K. J., MAYNE, J. R. (1975) J. Indust. Aero. 1, 167.

ENGINEERING SCIENCES DATA UNIT (1972, 1974) Data Sheets 72026, 74031.

FAGE, A., (1936) Proc. Roy. Soc. A 155, 570.

GOLDSTEIN, S. (1936) Proc. Roy. Soc. A 155, 576.

TOOMRE, A. (1960) Aero. Res. Coun. Rep. 22010 (FM 2872)

WOOD, C. J., (1977) Oxford Univ. Eng. Lab. Report 1188/77.

WOOD, C. J., (1977) Paper in preparation.